Neutron stars and matter at extreme conditions

中性子星と物質の極限状態

Kei Iida (Kochi University)

Contents

- *Neutron stars and pulsars: Mass, radius, etc.*
- *Dense nuclear matter: Introduction and recent topics*
- *Towards real EOS: Astronomical observations vs. lattice QCD*

Ref. Iida & Oyamatsu, EPJA **50** (2014) 42.

My earlier works…

Neutron drip line

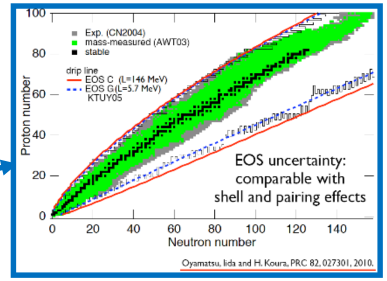

NS crustal torsional oscillations

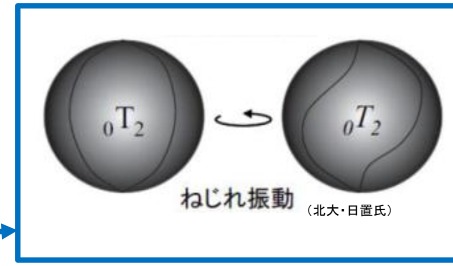

Mass & radius of n-rich nuclei

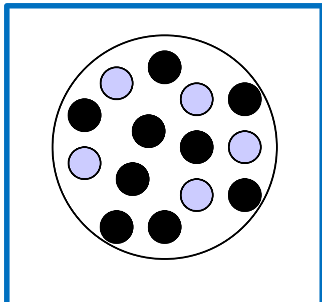

EOS of nuclear matter

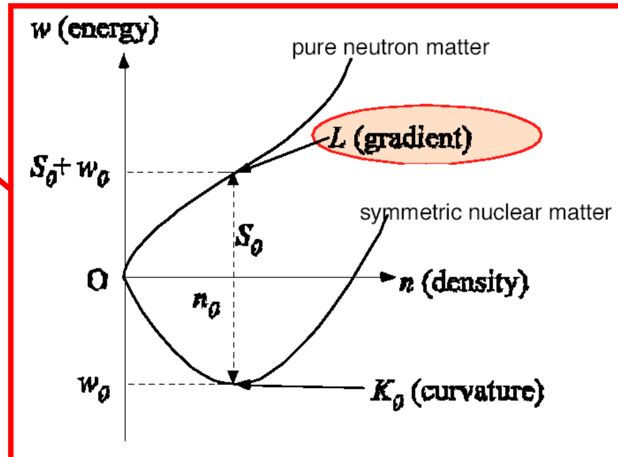

Mass & radius of light NSs

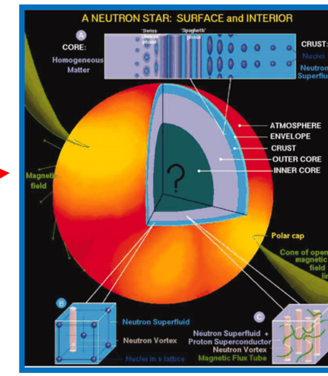

Black-sphere model for nuclei

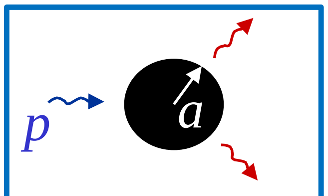

Reaction cross section formula

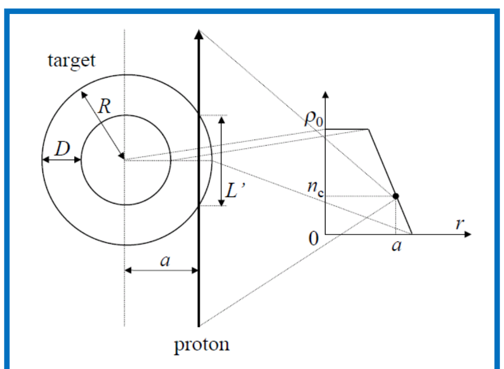

Incorporated in PHITS

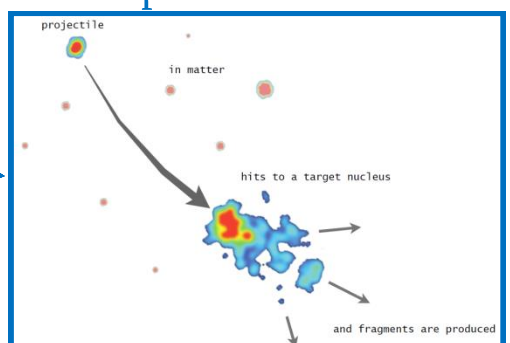

Nuclear pasta in NS crusts

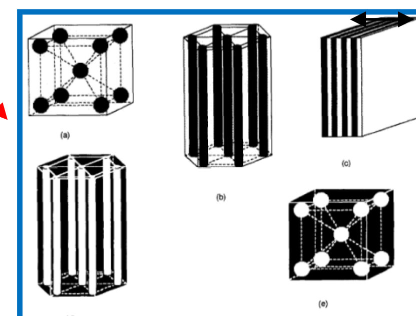

Neutron stars and pulsars

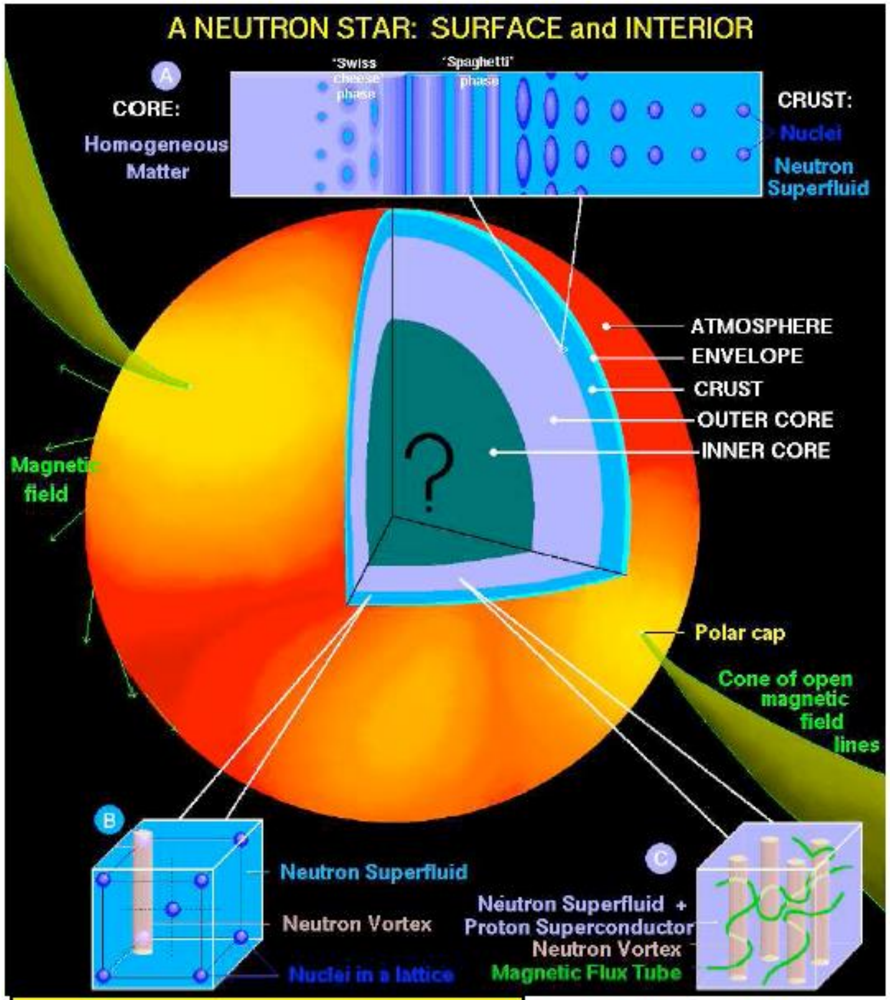

Lattimer and Prakash, astro-ph0405262

Figure by D. Page

Discovery of pulsars and neutron star observations

In 1967, Hewish & Bell discovered a "pulsar" emitting periodic radio pulses, PSR B1919+21 (at that time, referred to as LGM "Little Green Men"-1.)

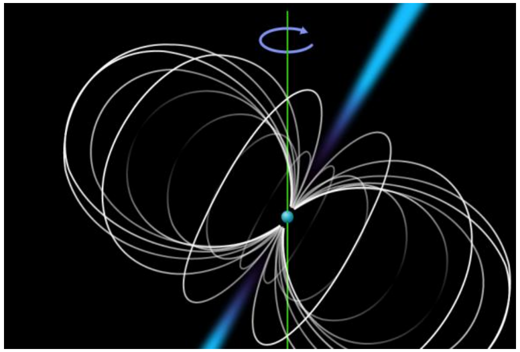

Imaginary drawing of a pulsar (gigantic "dynamo")

1968: A pulsar discovered in the Crab Nebula.

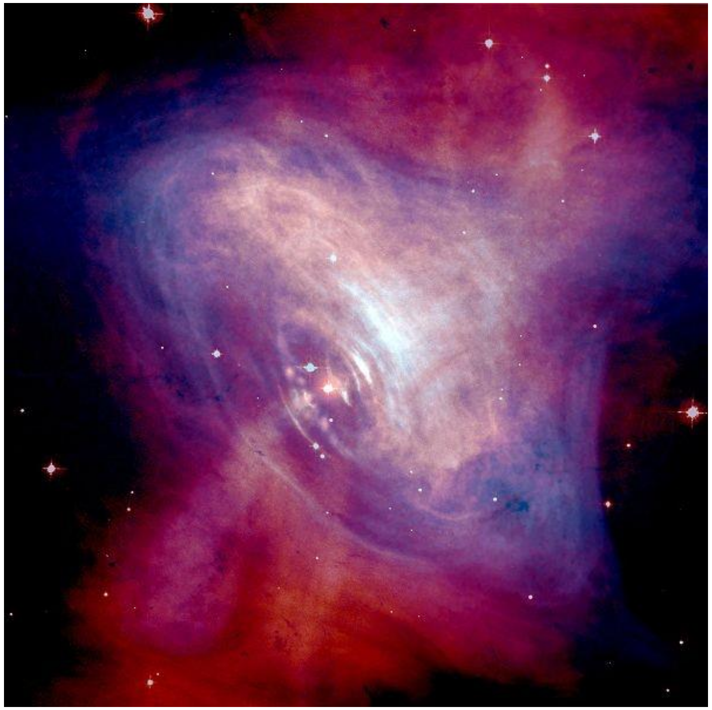

Crab Nebula (NASA/ESA)

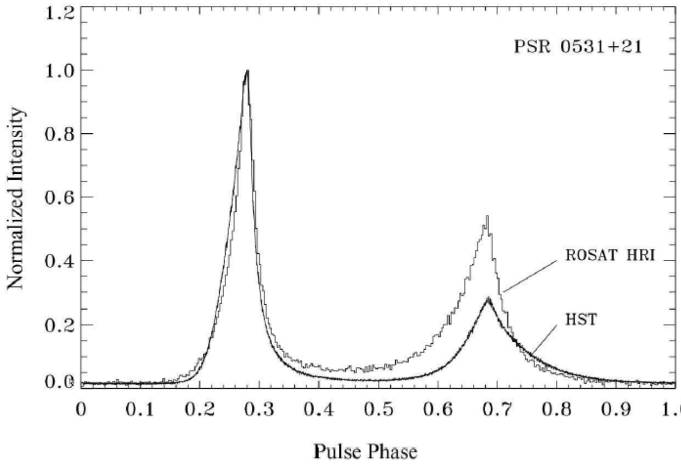

The very short (33 msec) period of the Crab pulsar helped to identify pulsars as neutron stars!

Pulsar glitch

From young pulsars, glitches, sudden decrease in the pulse period, are frequently observed.

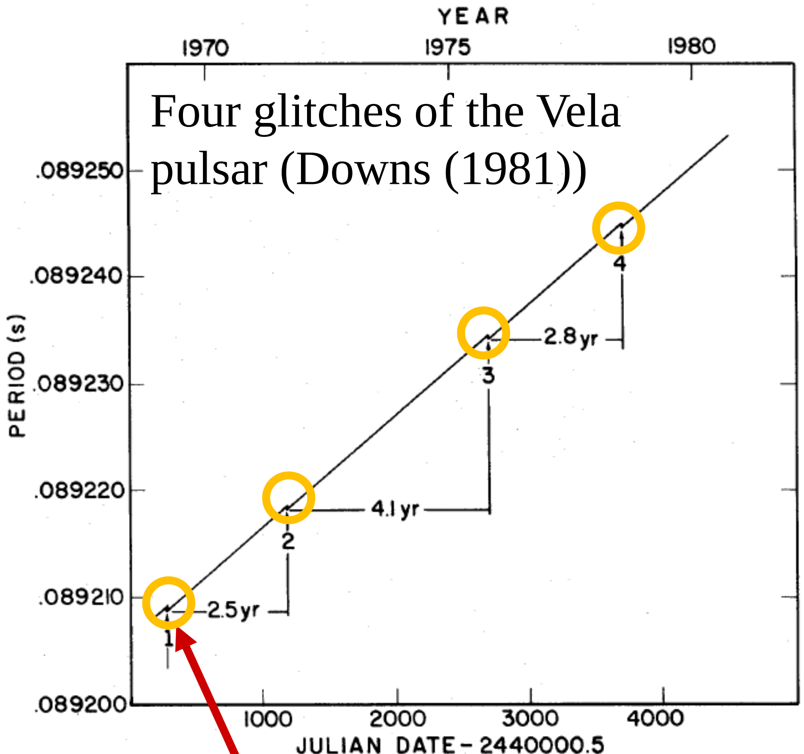

Four glitches of the Vela pulsar (Downs (1981))

Consistent with backreaction to disappearance of outwardly moving vortices, suggesting that superfluidity should occur in a neutron star!

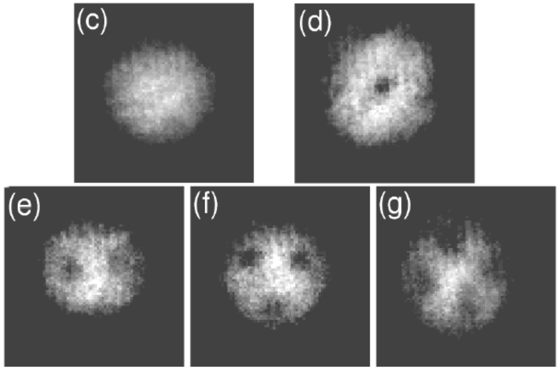

Vortices in rotating Bose condensate of Rb atoms (Madison et al.(2000))

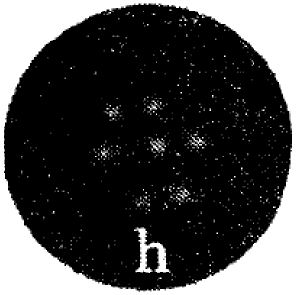

Vortices in rotating superfluid helium (Yarmchuk et al.(1979))

Neutron star mass determination by Hulse & Taylor

A pulsar with a binary companion:
Observed orbital motion → mass measurement!

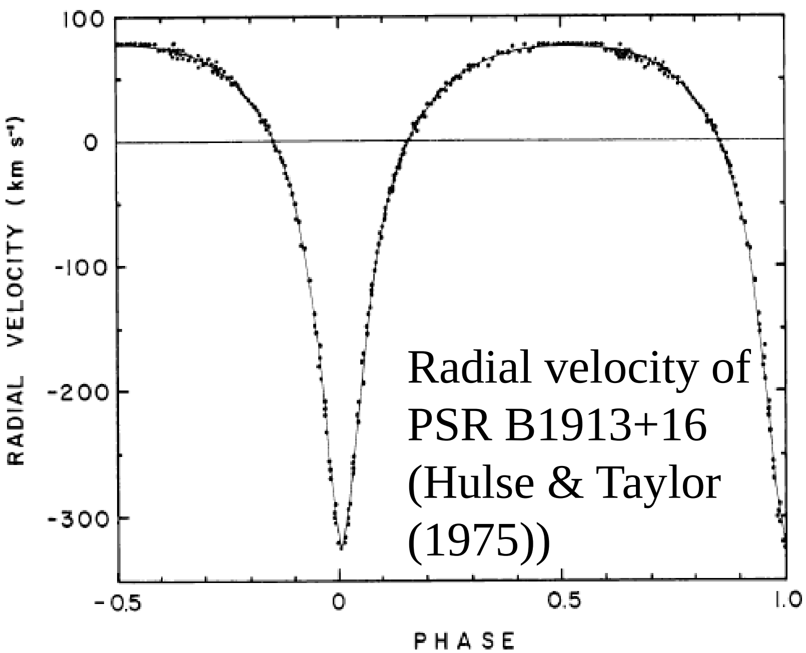

Radial velocity of PSR B1913+16 (Hulse & Taylor (1975))

The companion of PSR B1913+16 is also a neutron star!

⇩

Post-Keplerian orbit!

⇩

General relativity allows accurate mass determination!

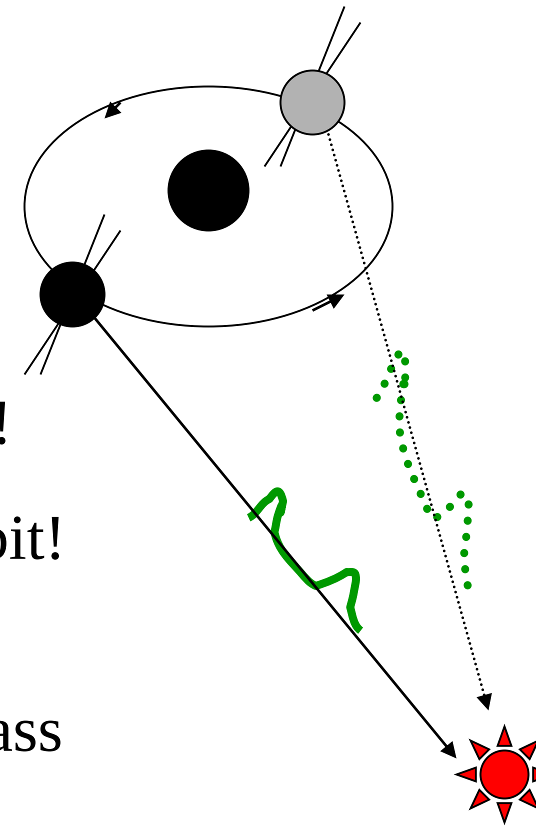

Neutron star–neutron star binaries

1518+49	$1.56^{+0.13}_{-0.44}$	(88)	1518+49 companion	$1.05^{+0.45}_{-0.11}$	(88)
1534+12	$1.3332^{+0.0010}_{-0.0010}$	(88)	1534+12 companion	$1.3452^{+0.0010}_{-0.0010}$	(88)
1913+16	$1.4408^{+0.0003}_{-0.0003}$	(88)	1913+16 companion	$1.3873^{+0.0003}_{-0.0003}$	(88)
2127+11C	$1.349^{+0.040}_{-0.040}$	(88)	2127+11C companion	$1.363^{+0.040}_{-0.040}$	(88)
J0737-3039A	$1.337^{+0.005}_{-0.005}$	(46)	J0737-3039B	$1.250^{+0.005}_{-0.005}$	(46)

Mean $= 1.34\ M_\odot$, weighted mean $= 1.41\ M_\odot$

Lattimer & Prakash (2004)

Neutron star mass determination by Hulse & Taylor (contd.)

Observed decrease in the orbital period was successfully explained by emission of gravitational waves predicted by general relativity.

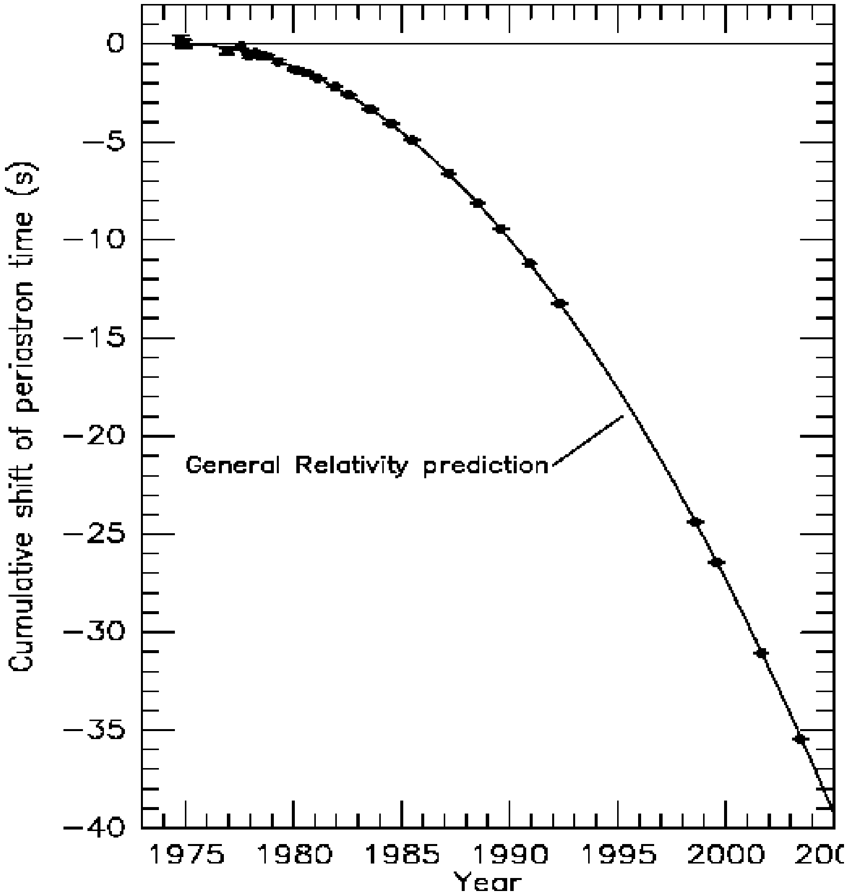

Decreasing orbital period of PSR B1913+
(Weisberg & Taylor (2004))

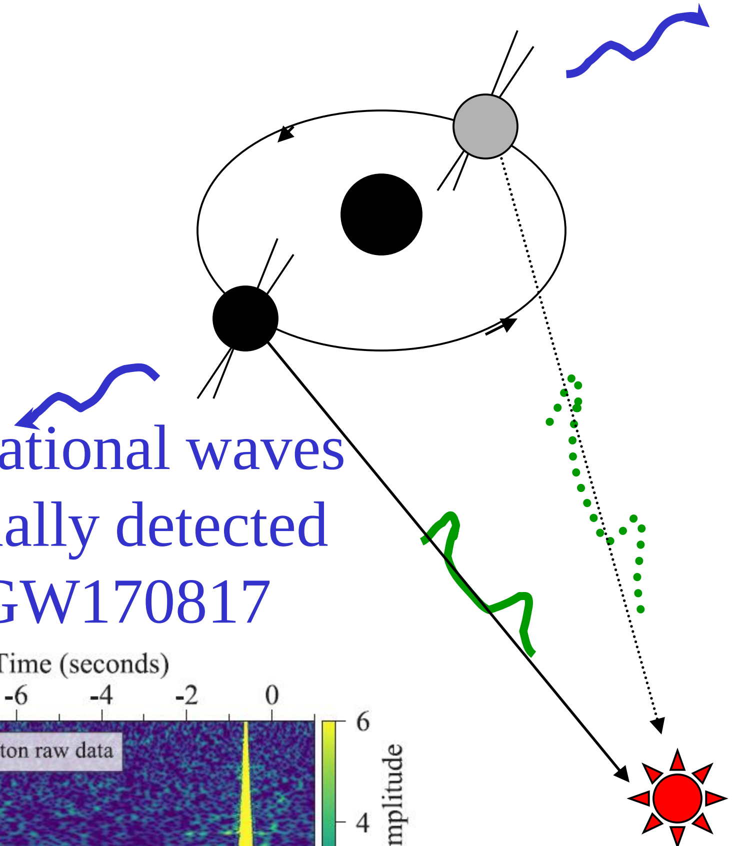

Gravitational waves eventually detected from GW170817

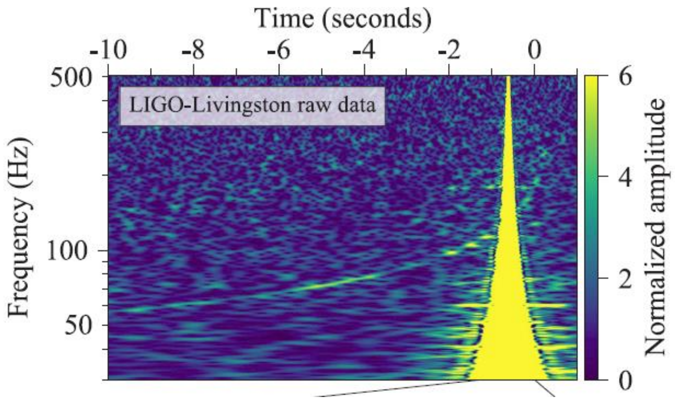

LIGO-Livingston (2017)

Neutron stars as theoretical products

▪1932: Discovery of the neutron by Chadwick via $^{9}\text{Be} + \alpha \rightarrow {}^{12}\text{C} + n$.

Just before that, Landau considered the possible presence of dense stars like one giant nucleus, and afterwards the possibility that a "neutron star" could exist due to the degeneracy pressure of neutrons of density higher than normal nuclear density.

▪1934: W. Baade and F. Zwicky, Phys. Rev. **45**, 138 (1934).

… With all reserve we advance the view that supernovae represent the transitions from ordinary stars into ***neutron stars***, which in their final stages consist of extremely closely packed neutrons.

Neutron stars as theoretical products (contd.)

Neutron star structure

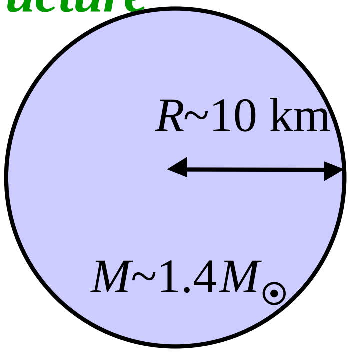

Neutron Fermi degeneracy pressure vs. gravity

$$P = \frac{2}{5} E_F n_n, \quad \text{where} \quad E_F = \frac{\hbar^2 k_F^2}{2m_n}, \quad k_F = \left(3\pi^2 n_n\right)^{1/3}$$

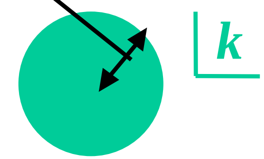

Why neutron-rich?

Stable nuclei: $Z \sim N$, basically no electrons inside

Neutron stars: Stellar remnants of gravitational collapse of massive stars

→ Mainly composed of neutrons, protons, and electrons that ensure charge neutrality

→ Each nucleon finds electrons in its vicinity.

→ μ_e makes matter neutron-rich via

$$p + e^- \to n + \nu_e$$

Chemical eq.

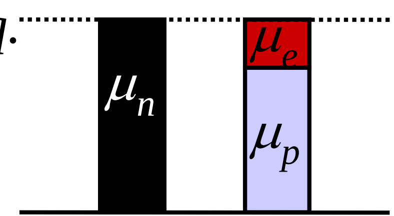

Matter in neutron stars

Schematic cross-section of a neutron star

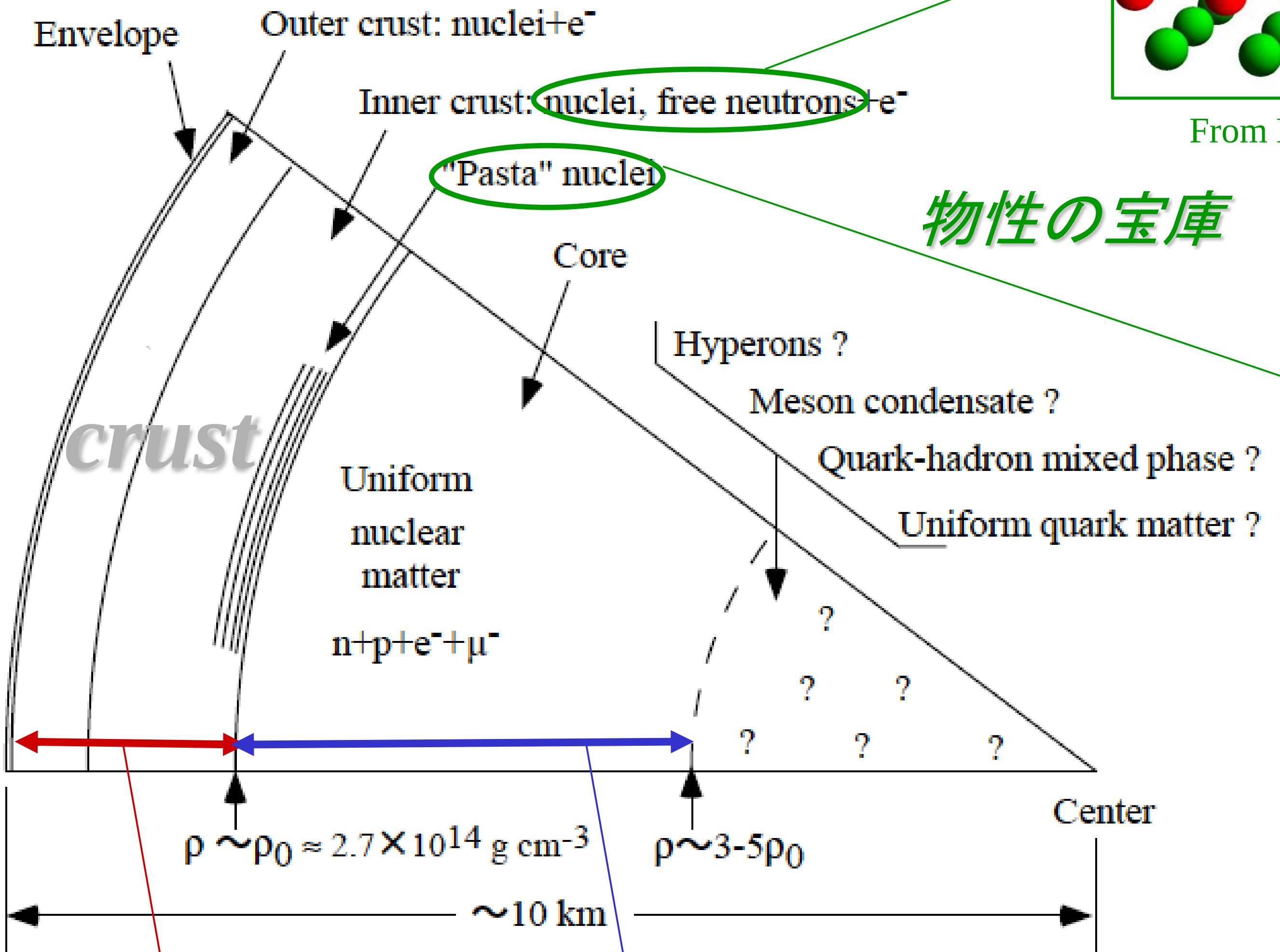

Liquid-gas mixture

Liquid

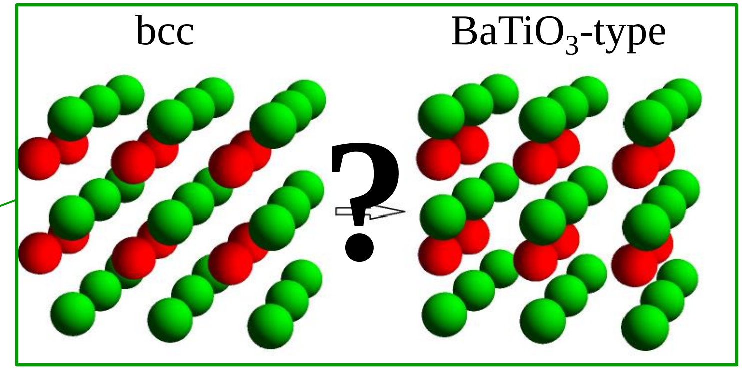

From Kobyakov and Pethick (2013, 2016).

物性の宝庫

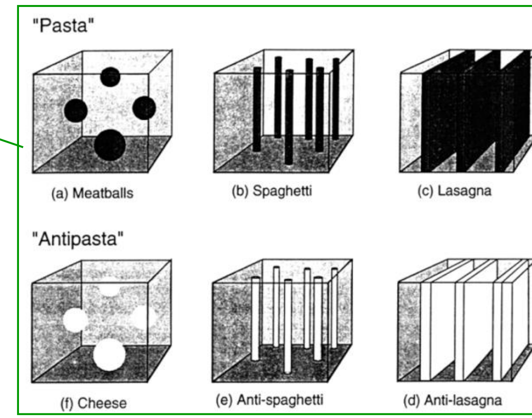

From Lamb (1991).

$T <\sim 10^9$ K（cold）

Matter in neutron stars (contd.)

閉じ込められていた粒子の解放（ゼロ温度の場合）

密度 (g cm^{-3})

原子・分子固体

1 水素物質の場合地球の中心圧力に相当

高密度（圧力電離）プラズマ

電子とイオン（原子核）

10^{14} 原子核の内部密度

核物質

電子と核子（陽子や中性子）

10^{15} 中性子星の中心密度

クォーク物質？

電子とクォーク

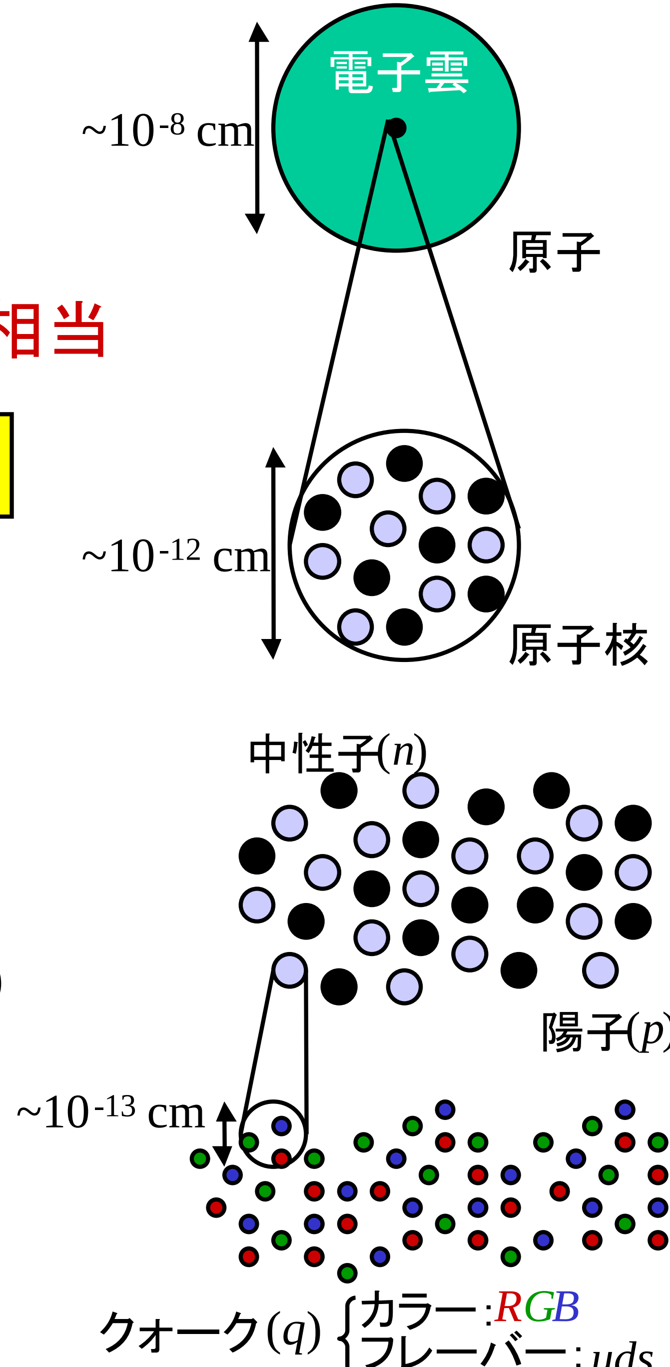

Mass-radius relation of light neutron stars

Combining
$$\frac{dP}{dr} = -\frac{G[\rho(r)+P(r)/c^2][m(r)+4\pi r^3 P(r)/c^2]}{r^2[1-2Gm(r)/rc^2]}$$
$$m(r) = \int_0^r \rho(r) 4\pi r^2 dr$$
& EOS models for neutron star matter

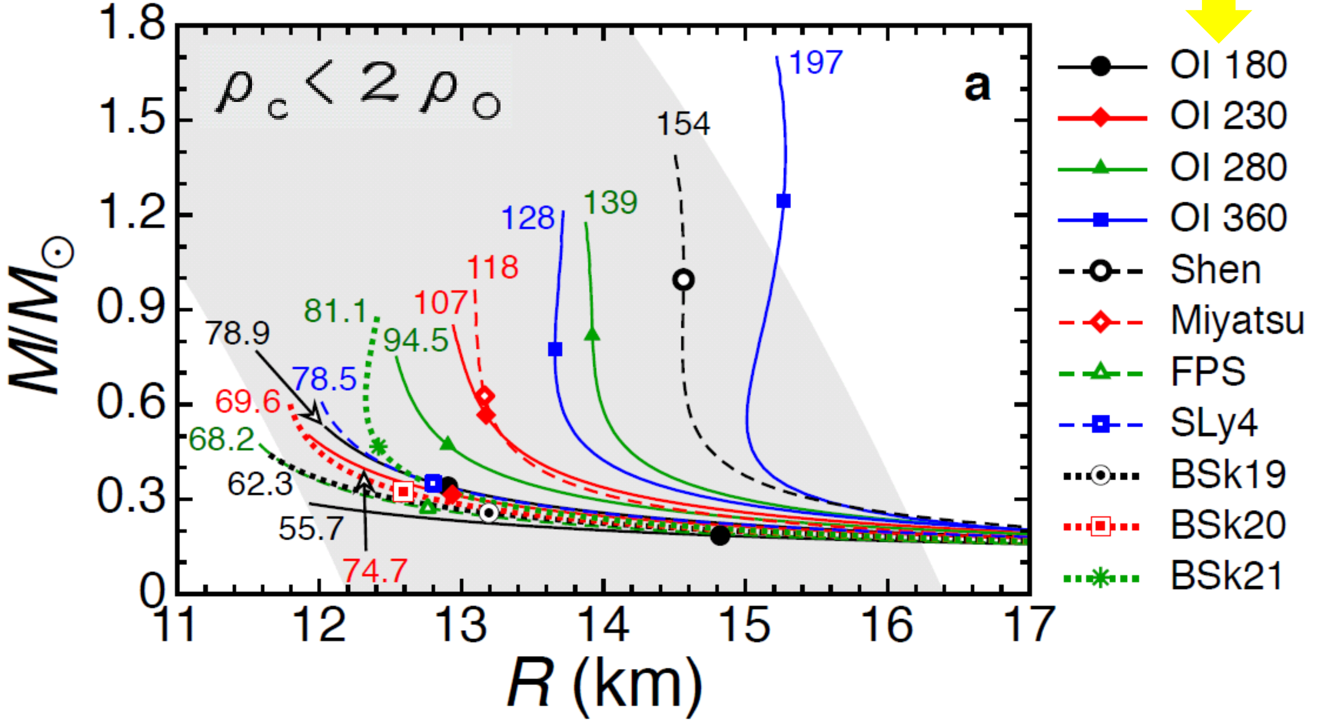

Sotani, Iida, Oyamatsu, & Ohnishi, arXiv:1401.0161.

In contrast,

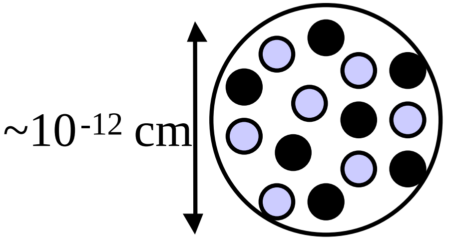

Atomic nucleus

$M \propto R^3$

Multimessenger observations of GW170817

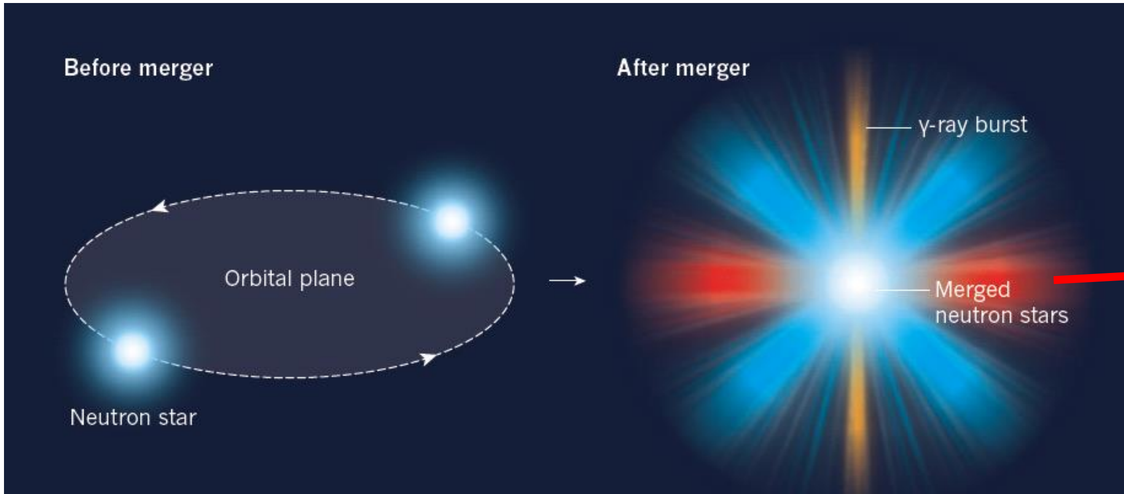

Coleman Miller (Nature **551** (2017) 36)

Heavy elements produced

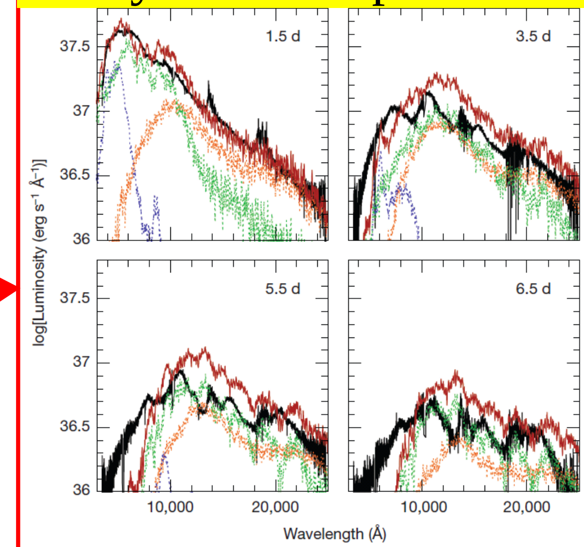

Figure 3 | Kilonova models compared with the AT 2017gfo spectra.

Pian et al. Nature **551,** 67 (2017).

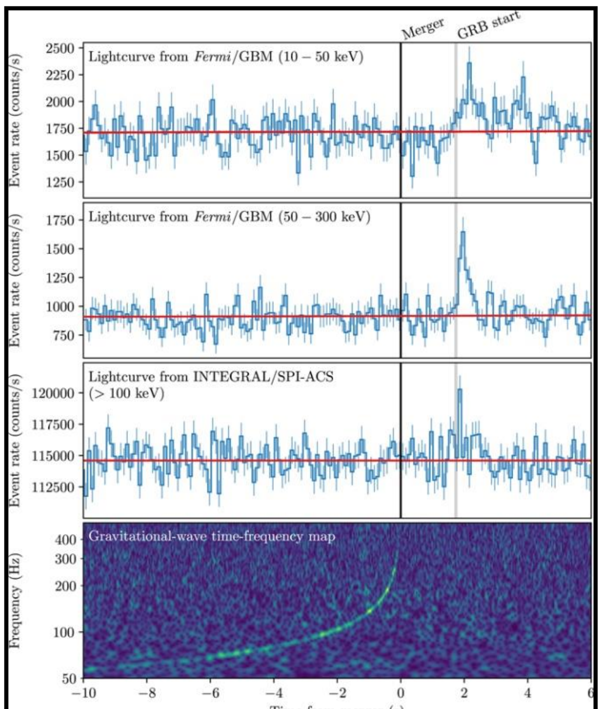

Inspiral phase

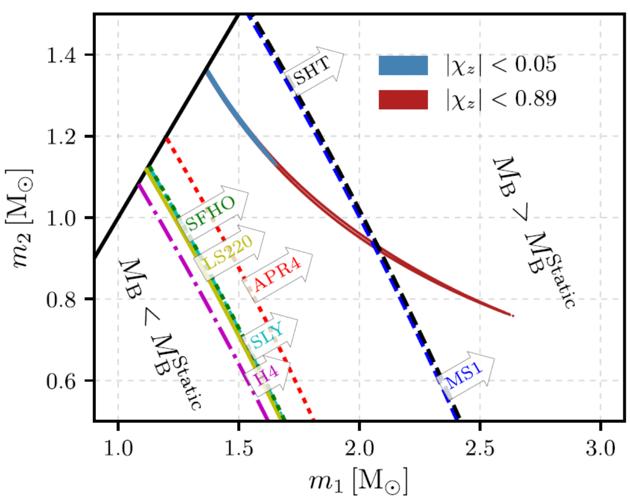

Late inspiral phase

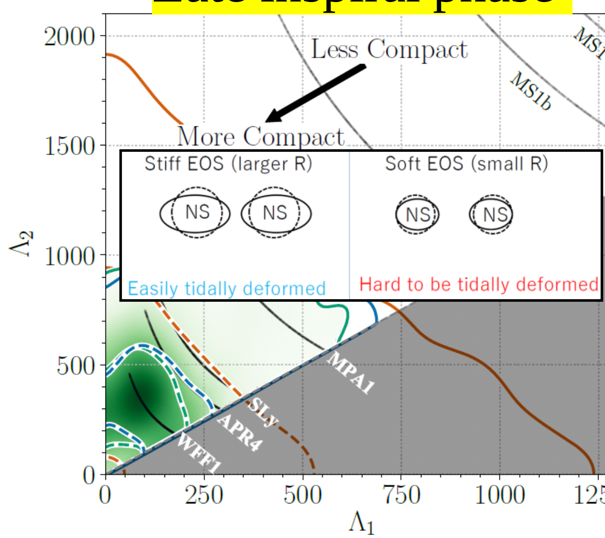

$$\Lambda \equiv \frac{2}{3}k_2^{(\mathrm{tid})}\left(\frac{Rc^2}{GM}\right)^5$$

Abbott et al. ApJ **848,** L13 (2017); LIGO & Virgo PRL **121**, 161101 (2018); K. Kiuchi et al. (2018)

Constraints from GW170817

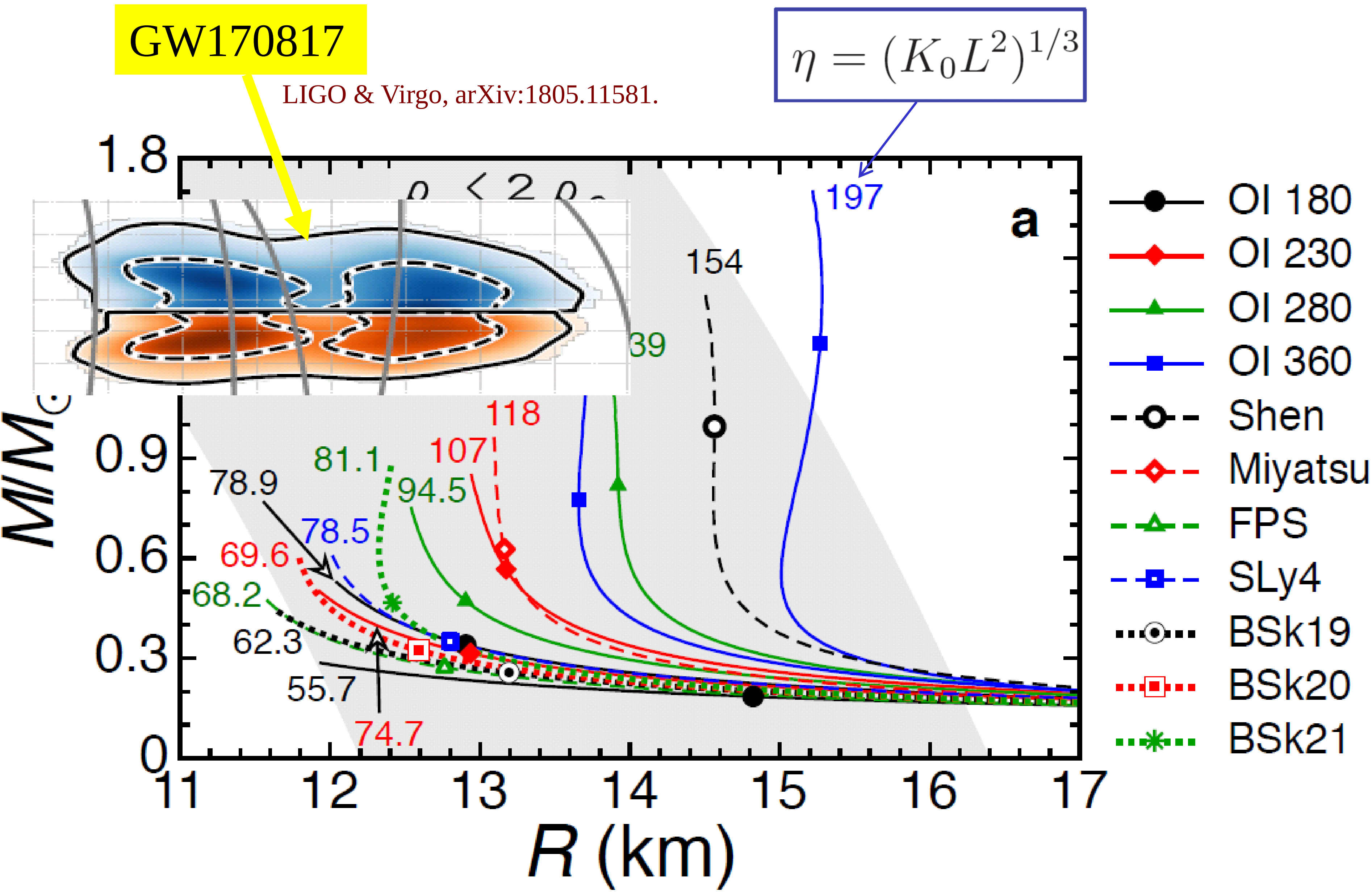

Sotani, Iida, Oyamatsu, & Ohnishi, arXiv:1401.0161.

Observed masses

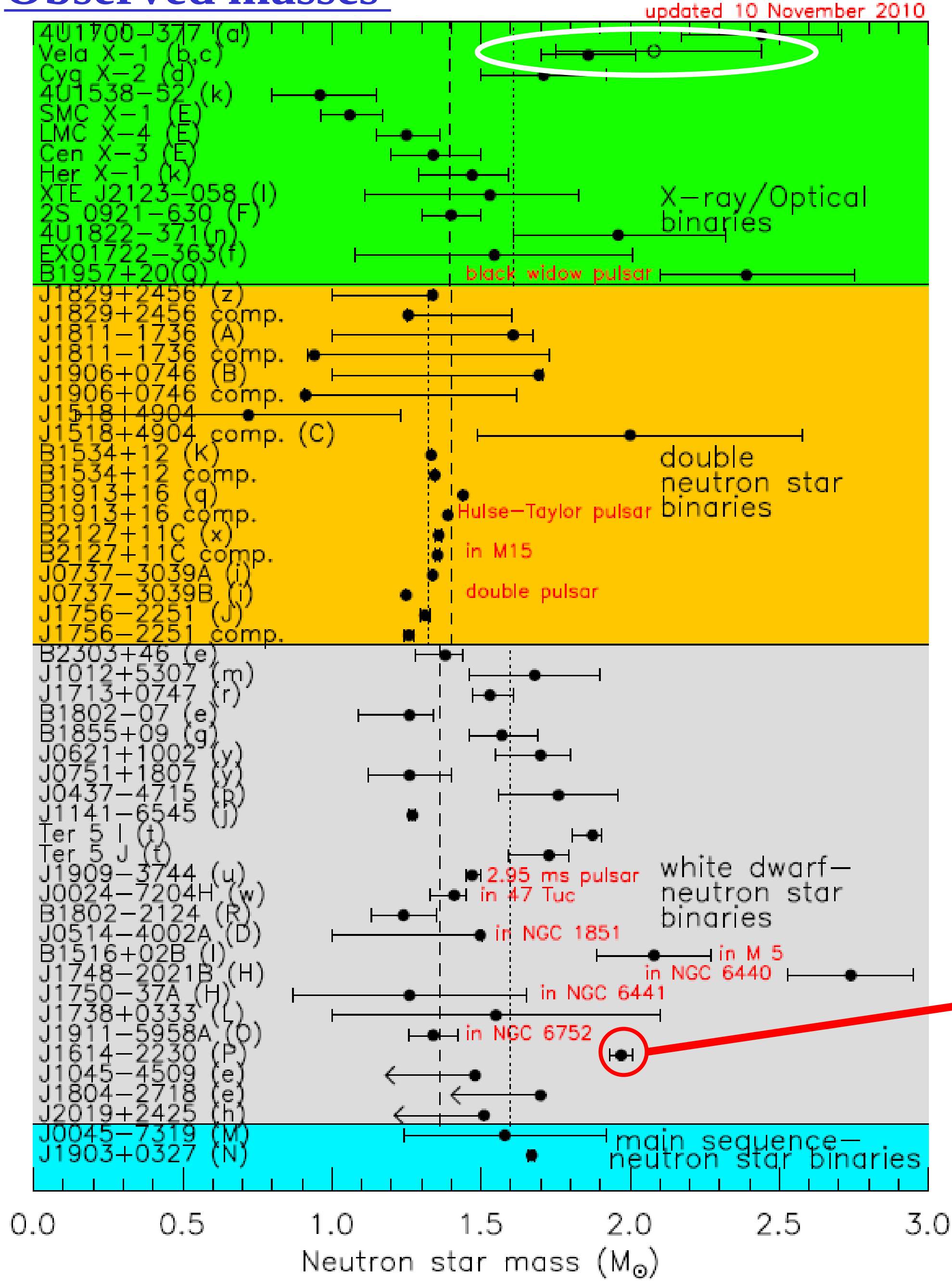

Lattimer & Prakash, arXiv:1012.3208.

Pulsar twice as heavy as the Sun

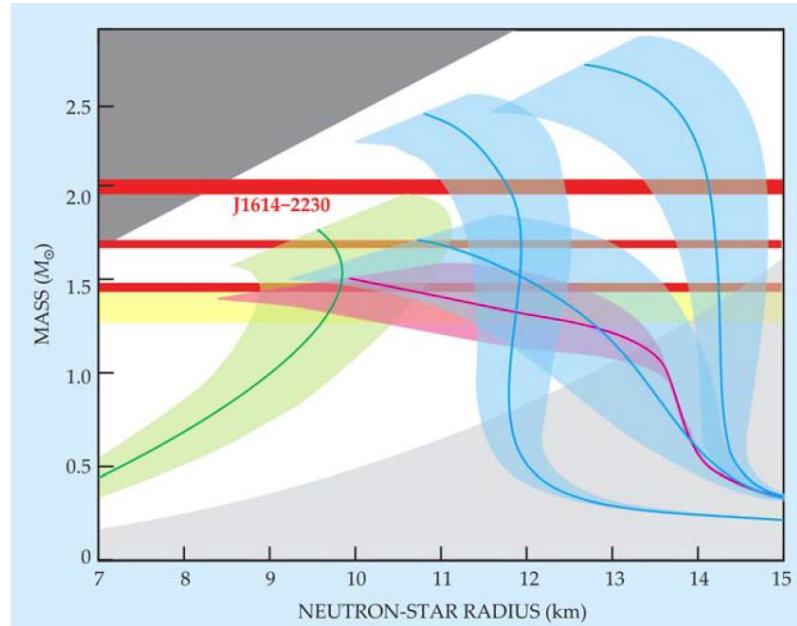

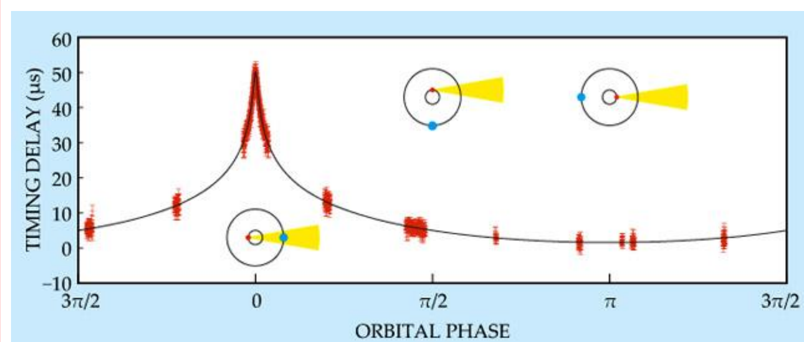

Demorest et al. (2010)

The Best Measured Neutron Star Radii

Name	R_∞ (km/D)	D (kpc)	$kT_{eff,\infty}$ (eV)	N_H (10^{20} cm^{-2})	Ref.
omega Cen (Chandra)	13.5 ± 2.1	5.36 ±6%	66^{+4}_{-5}	(9)	Rutledge et al (2002)
omega Cen** (XMM)	13.6 ± 0.3	5.36 ±6%	67 ± 2	9 ± 2.5	Gendre et al (2002)
M13** (XMM)	12.6 ± 0.4	7.80 ±2%	76 ± 3	(1.1)	Gendre et al (2002)
47 Tuc X7 (Chandra)	34_{-13}^{+22}	5.13 ±4%	84^{+13}_{-12}	$0.13^{+0.06}_{-0.04}$	Heinke et al (2006)
M28** (Chandra)	$14.5_{-3.8}^{+6.9}$	5.5 ±10%	90_{-10}^{+30}	26 ± 4	Becker et al (2003)
M30 (Chandra)	$16.9_{-4.3}^{+5.4}$	--	94_{-12}^{+17}	$2.9^{+1.7}_{-1.2}$	Lugger et al (2006)
NGC 2808 (XMM)	??	9.6 (?)	103_{-33}^{+18}	18^{+11}_{-7}	Webb et al (2007)

$$\boxed{R_\infty < 5\%}$$

Caveats:

- All IDd by X-ray spectrum (47 Tuc, Omega Cen now have optical counterparts)
- calibration uncertainties

Distances:
Carretta et al (2000),
Thompson et al (2001)

Quiescent low-mass X-ray binaries in globular clusters

Apparent radius:

$$R_\infty = \frac{R}{\sqrt{1-2GM/Rc^2}}$$

Distance to the globular cluster

Rutledge (2010)

Neutron star cooling

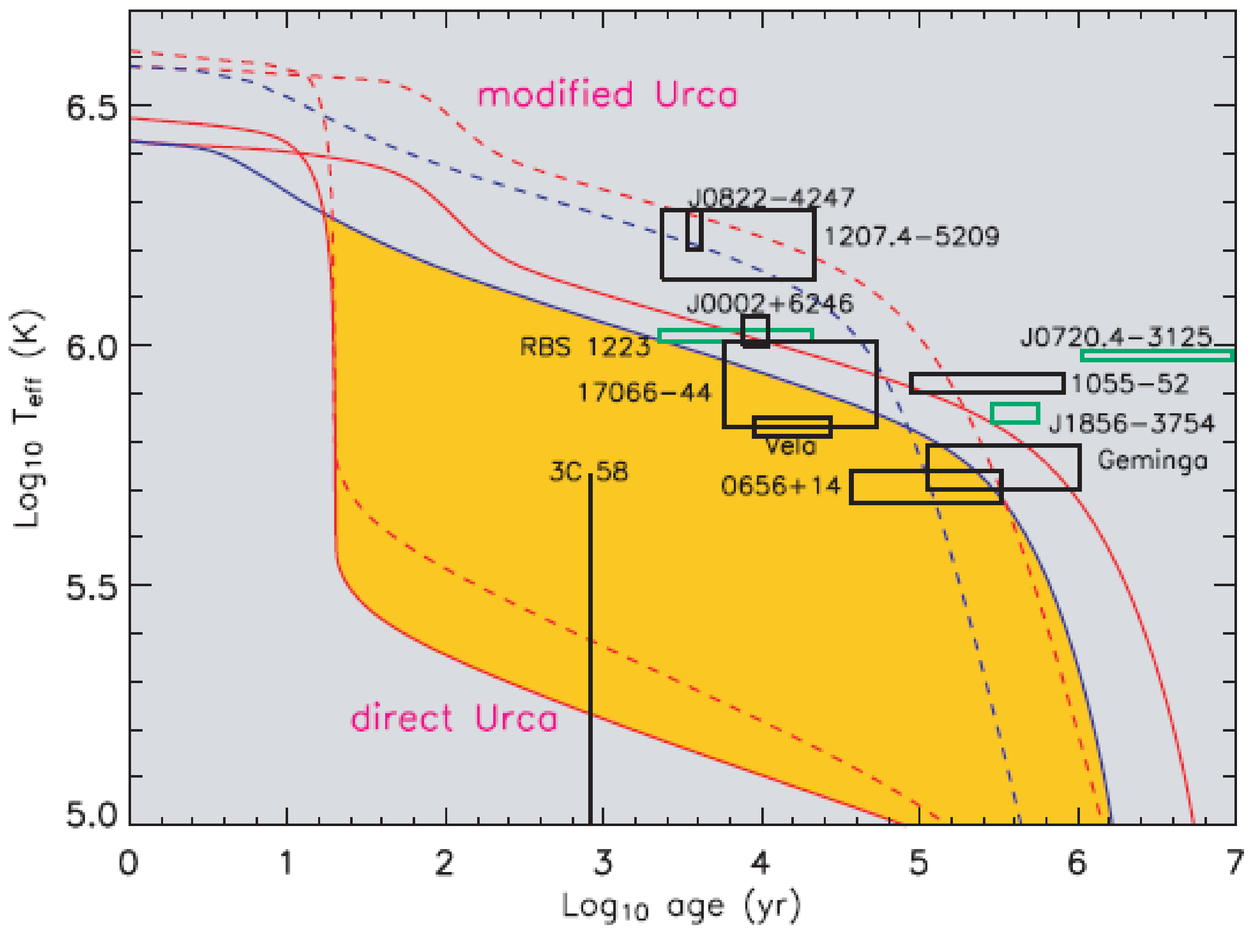

Fig. 4. Observational estimates of neutron star temperatures and ages together with theoretical cooling simulations for $M = 1.4\,M_\odot$. Models (solid and dashed curves) and data with uncertainties (boxes) are described in (*43*). The green error boxes indicate sources from which thermal optical emissions have been observed in addition to thermal x-rays. Simulations with Fe (H) envelopes are displayed by solid (dashed) curves; those including (excluding) the effects of superfluidity are in red (blue). The upper four curves include cooling from modified Urca processes only; the lower two curves allow cooling with direct Urca processes and neglect the effects of superfluidity. Models forbidding direct Urca processes are relatively independent of *M* and superfluid properties. The yellow region encompasses cooling curves for models with direct Urca cooling including superfluidity.

Lattimer & Prakash (2004)

Dense nuclear matter

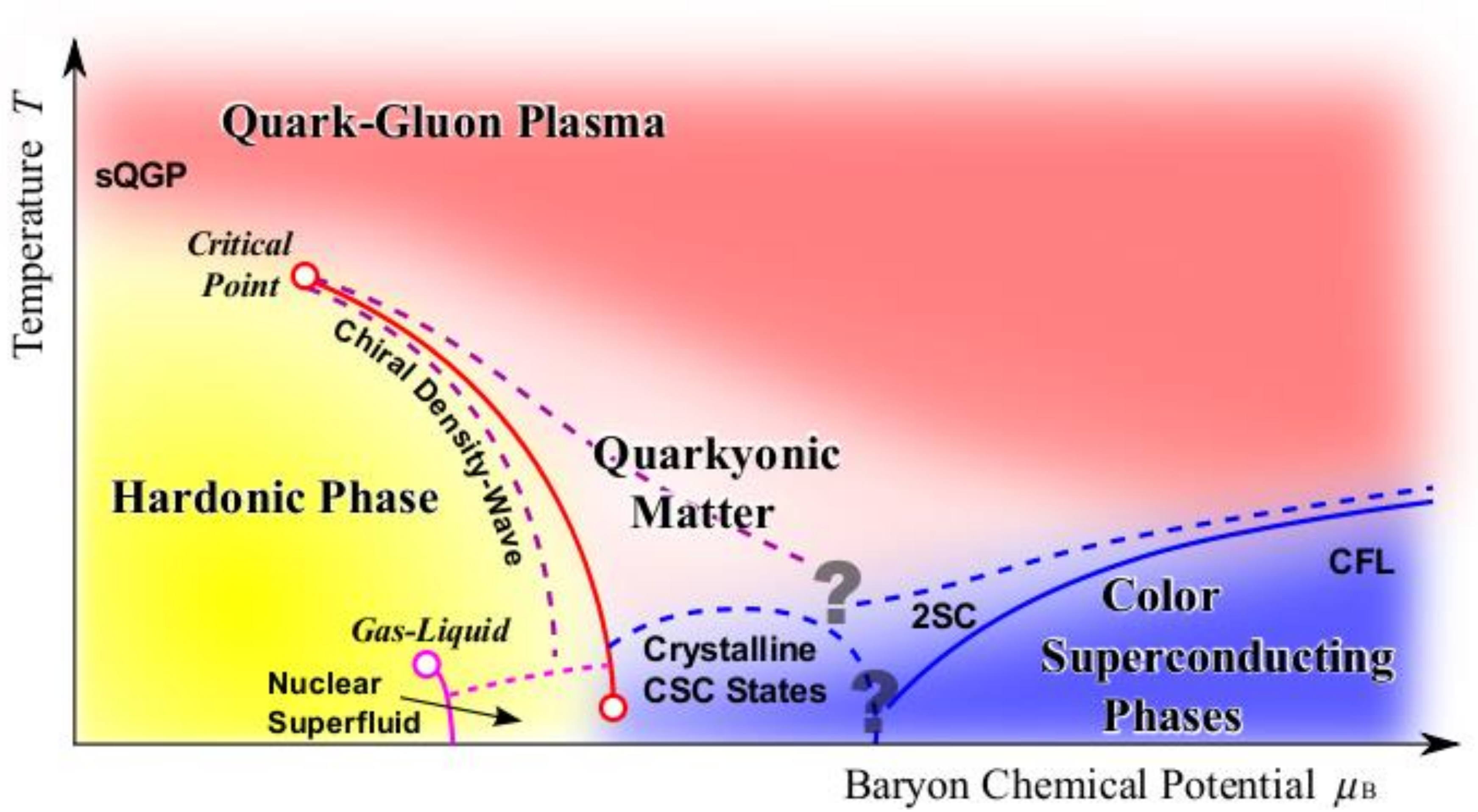

By Fukushima

Systems composed of nuclear matter

Ishii et al., PRL **99**(2007)022001.

核物質

真空中の核力の性質と起こりうる相転移

・核子散乱実験や重陽子の性質

・比較的遠方では π 交換

・近距離の性質はいまだ？
　クォークの影響は？

核子間ポテンシャル

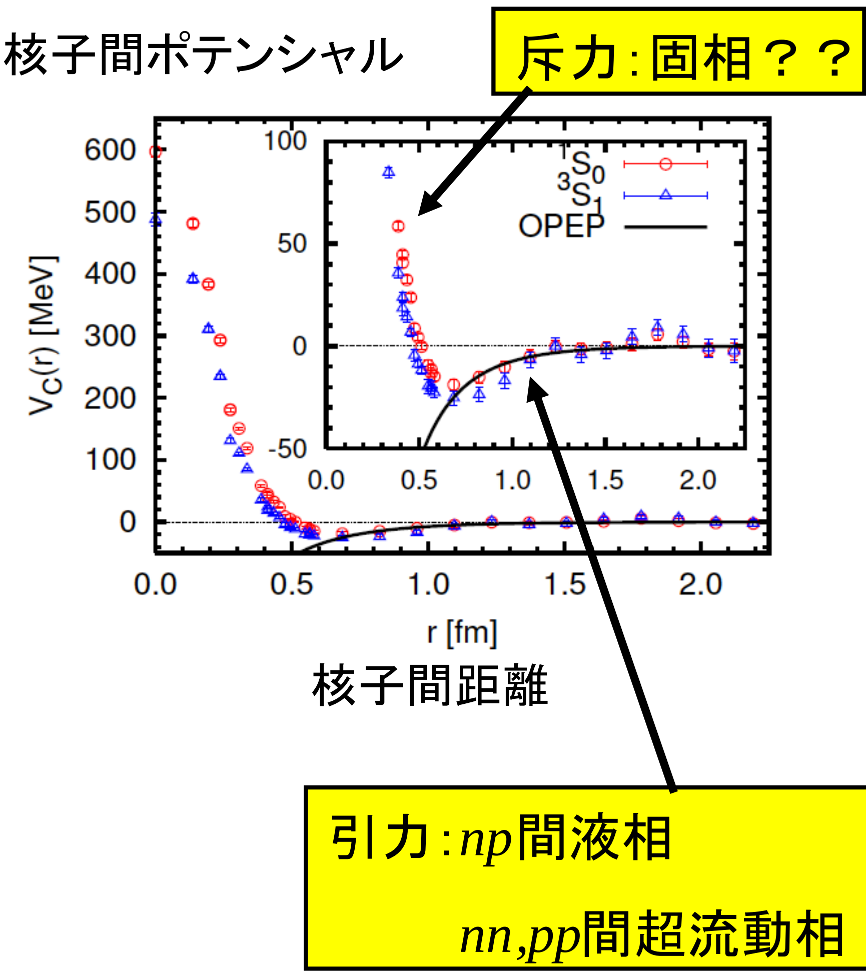

核子間距離

何処に？

・通常の核物質 —— 原子核

・高温高密度核物質、高温クォーク物質（？）—— 重イオン同士の衝突

・高密度核物質、高密度クォーク物質（？）—— 中性子星

Systems composed of nuclear matter (contd.)

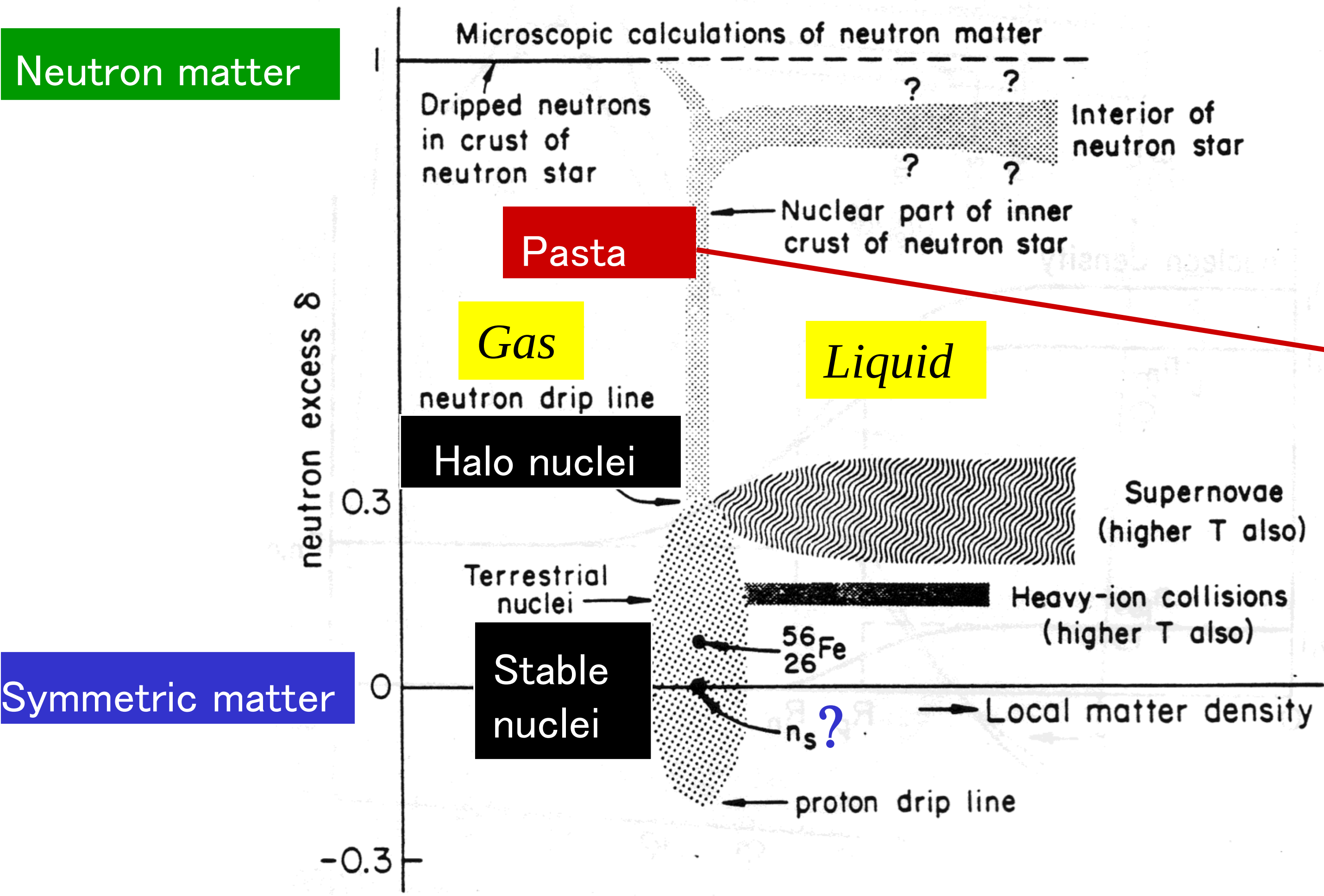

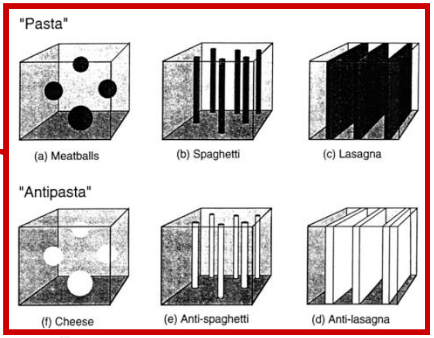

From Lamb (1991).

Pethick & Ravenhall, ARNPS **45** (1995) 429.

Microscopic EOS calculations

Pure neutron matter

Scattering length $a \approx$-18 fm
Effective range $\approx$2 fm

Green's function Monte-Carlo (GFMC) with Argonne v_8'

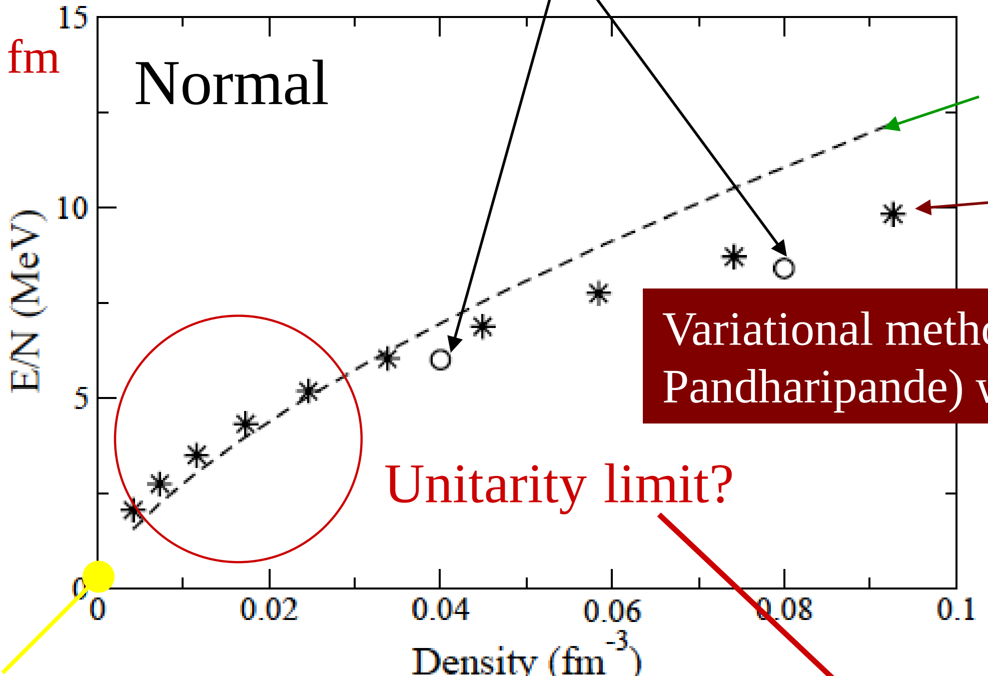

$0.5E_{FG}/N$

Variational method (Friedman-Pandharipande) with Urbana v_{14}+TNI

Unitarity limit?

$|a| >> k_F^{-1} >> R$

Low - density expansion :

$$E = E_{FG}\left[1 + \frac{10}{9\pi}k_F a + \frac{4}{21\pi^2}(11 - 2\ln 2)(k_F a)^2 + \ldots\right]$$

Ref. Carlson et al., PRC **68** (2003) 025802.

Symmetric nuclear matter

Variational method: Overbinding without phenomenological three-nucleon forces

Microscopic EOS calculations (contd.)

Pure neutron matter

Superfluid (Pairing) Gap

Polarization

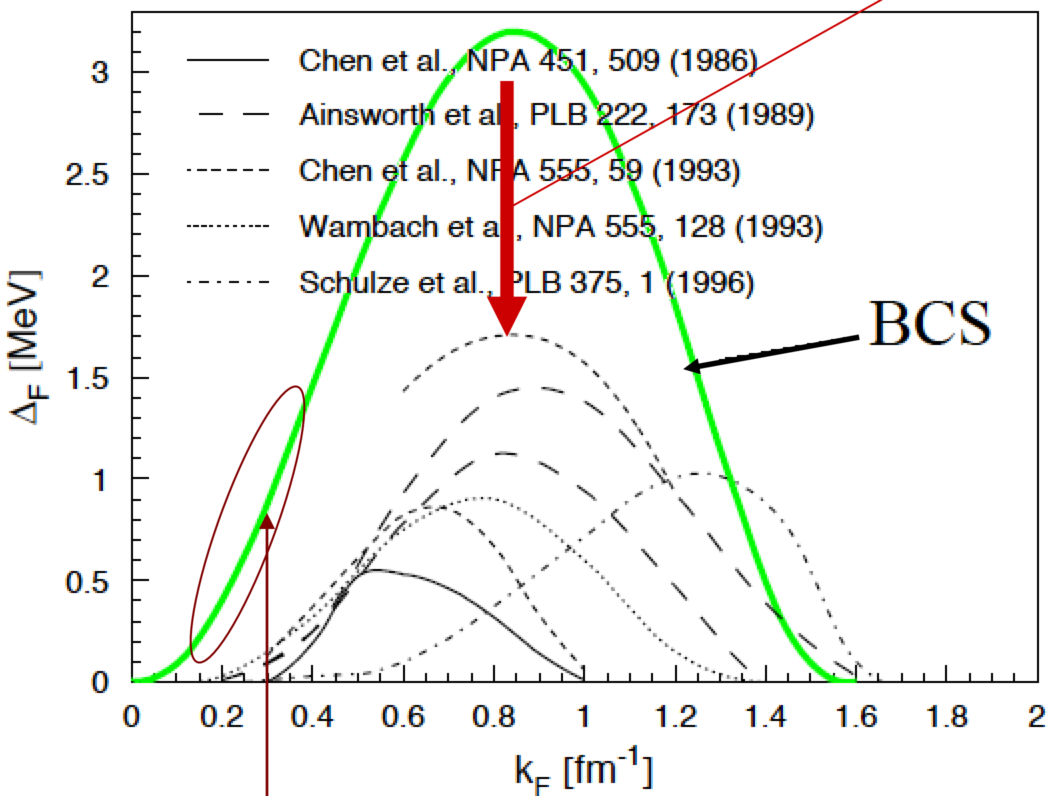

BCS

Dean and Hjorth-Jenson RMP (2003)

Uncertainties

large

small

Consistent

$$\text{Unitarity limit (by QMC)}: \ \Delta_F = 0.5(0.1)E_F$$

Ref. Carlson and Reddy, PRL **95** (2005) 060401.

Neutron matter and trapped cold atoms

Low density neutron matter

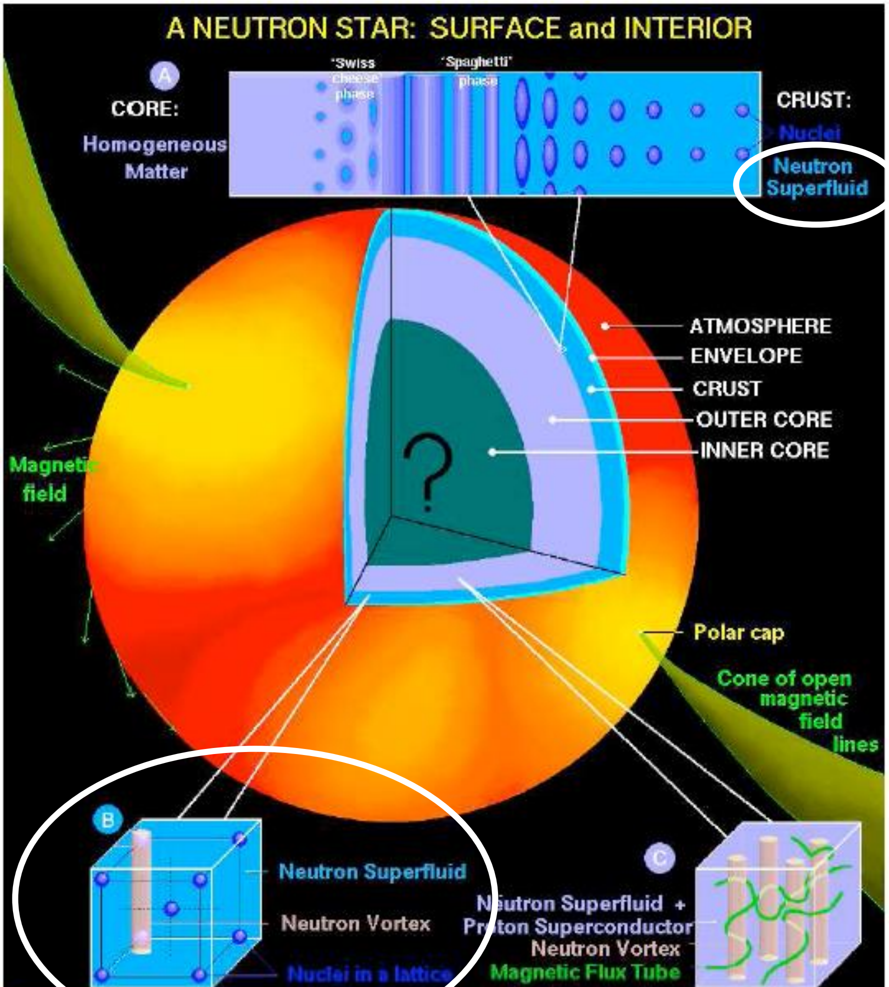

Lattimer and Prakash, astro-ph0405262

Figure by D. Page

Cold Fermi atoms near Feshbach resonance

Universal Interaction Energy at Unitarity

In-situ absorption images

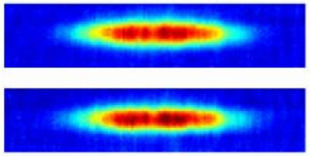

Size of real space distribution reveals interaction and pairing energies

At unitarity, the chemical potential is reduced by pairing: $\mu = E_F(1+\beta)^{1/2}$

where β is a *universal* many-body parameter $\beta = -0.54 \pm 0.05$

From R. Hulet.

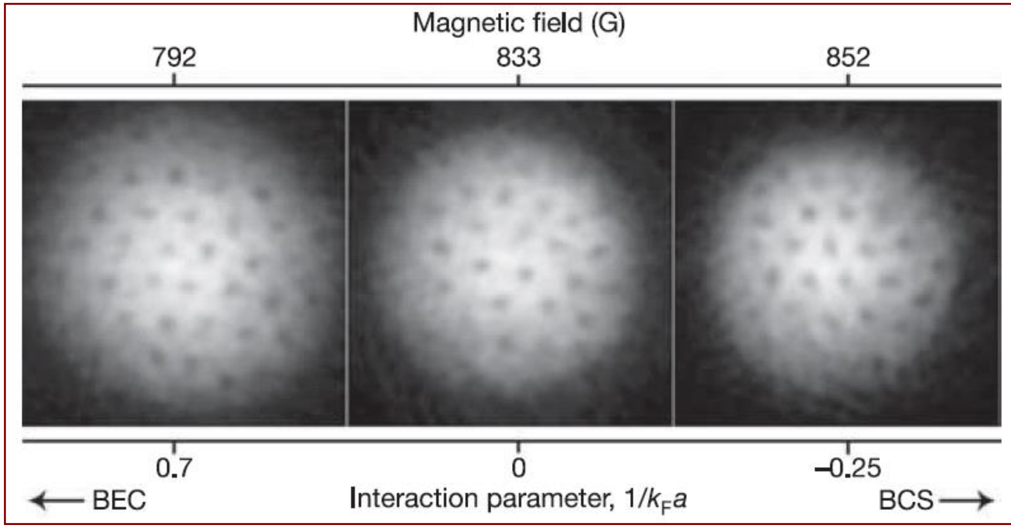

From M.W. Zwierlein.

Phenomenological EOS parameters

Energy per nucleon of bulk nuclear matter near the saturation point (nucleon density n, neutron excess α):

$$w = w_0 + \frac{K_0}{18n_0^2}(n-n_0)^2 + \left[S_0 + \frac{L}{3n_0}(n-n_0)\right]\alpha^2$$

n_0, w_0 saturation density & energy of symmetric nuclear matter

S_0 symmetry energy coefficient

K_0 incompressibility

L density symmetry coefficient

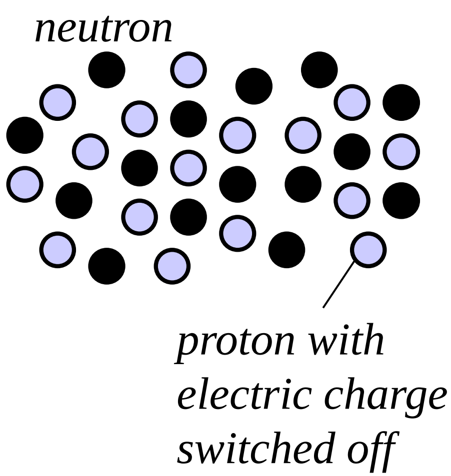

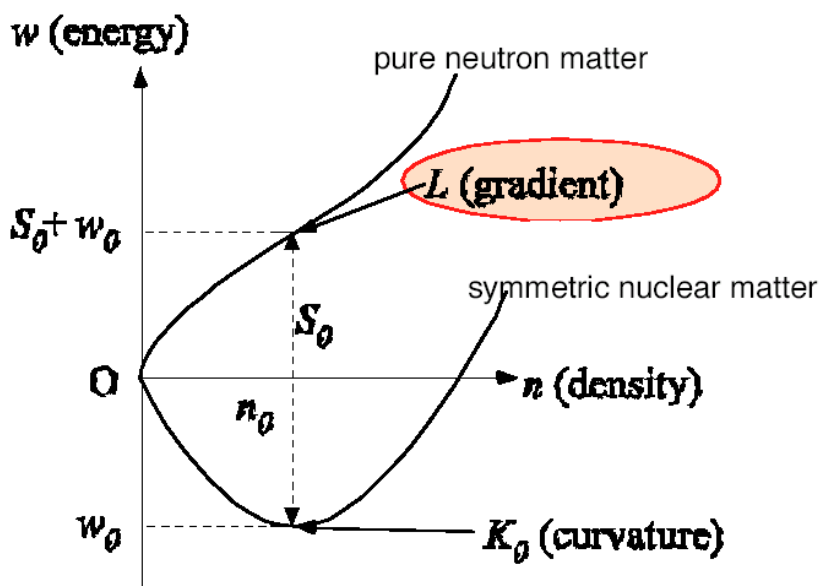

L is still uncertain, but controls various properties of neutron star crusts!

Phenomenological EOS parameters (contd.)

constraints on L

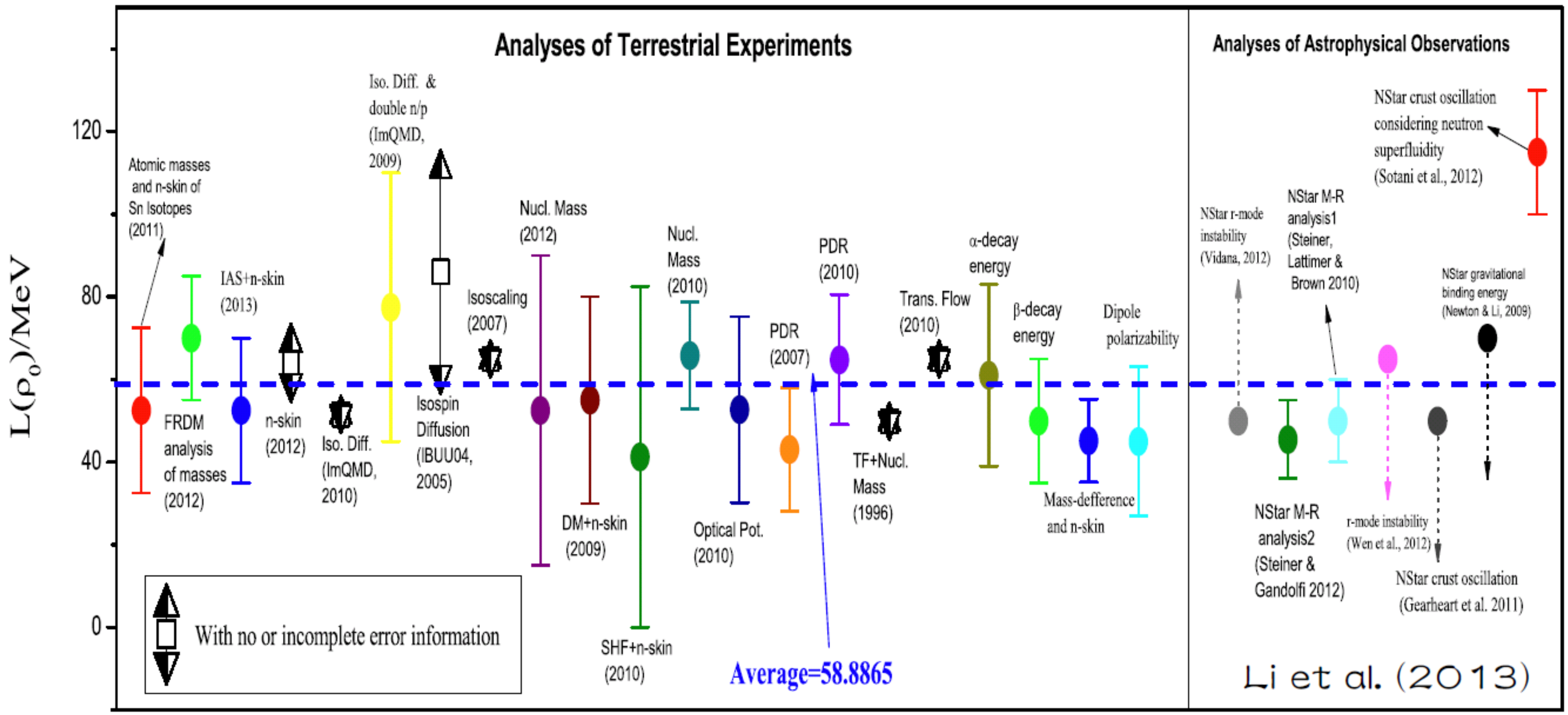

- most of constraints on L predict around $40 \lesssim L \lesssim 80$ MeV

OI EOS family

Zero-temperature EOS of uniform nuclear matter

Incompressibility (K_0)

Slope of the symmetry energy (L)

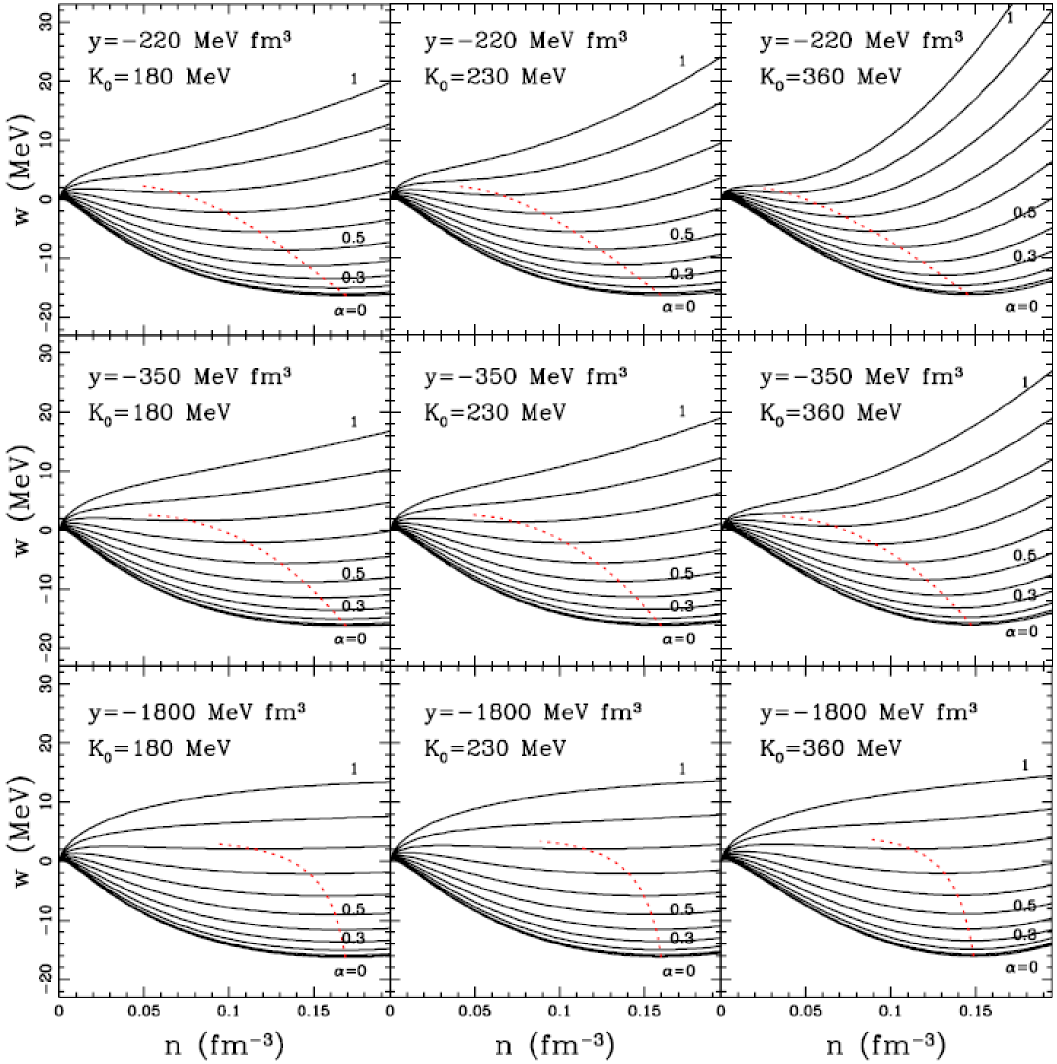

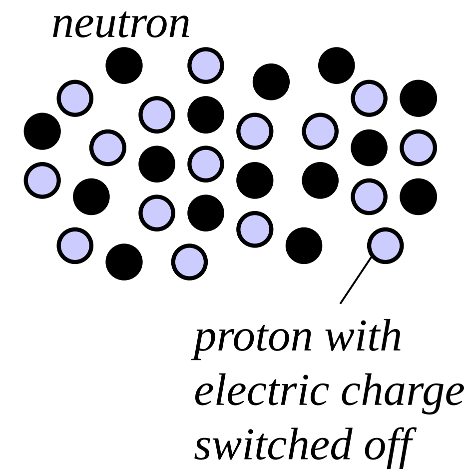

9 extreme cases:

・equally reproducing empirical data for masses & charge radii of stable nuclei

・could be selected from future data of unstable nuclei?

Ref. Oyamatsu & Iida, PTP **109** (2003) 631；Kohama, Iida, & Oyamatsu PRC **72** (2005) 024602.

Theoretical upper bound on the neutron star mass

Oppenheimer & Volkoff (1939) suggested that the mass of a stable neutron star becomes maximum for the stiffest possible equation of state that is consistent with fundamental physics.

Rhoades & Ruffini (1974) proved that, in the regions where it is uncertain, the equation of state that produces the maximum neutron star mass is the one for which the sound speed is equal to the speed of light.

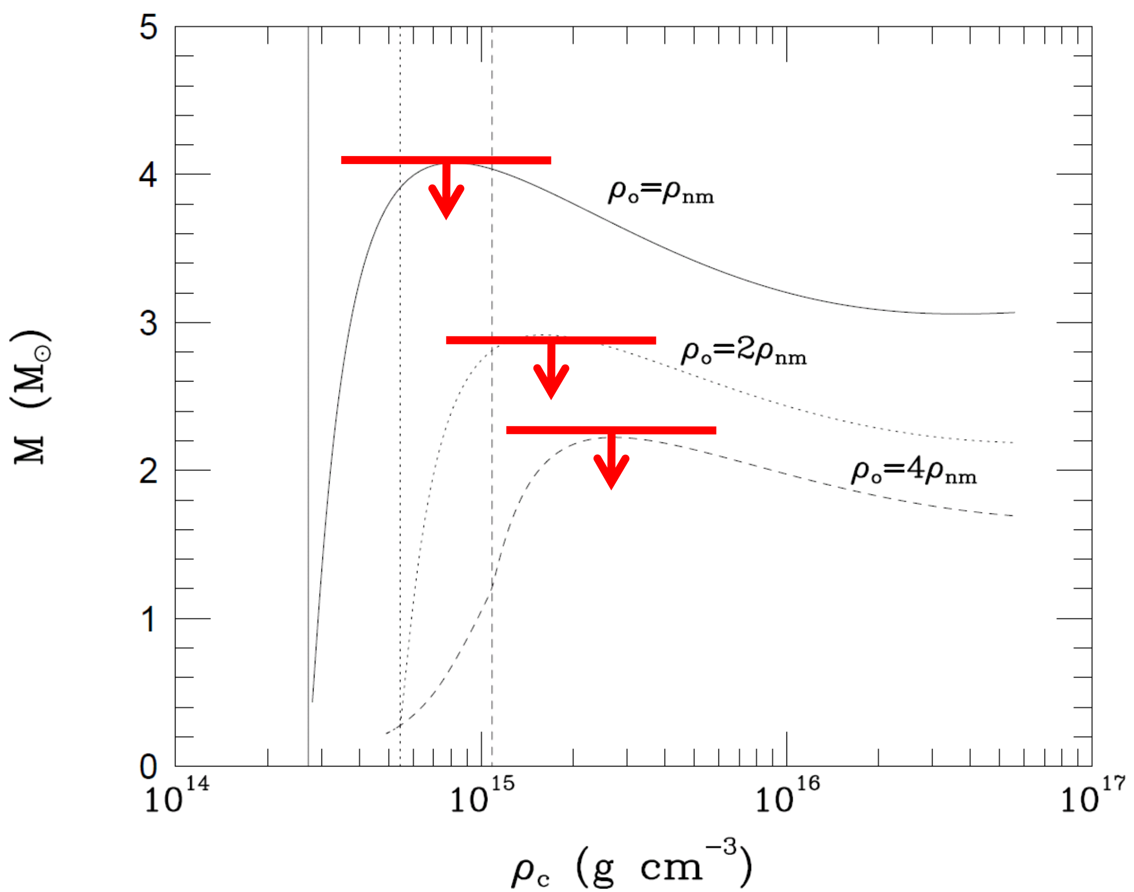

EOS

$\rho<\rho_O$: Wiringa et al. (1988)

$\rho>\rho_O$: sound speed = c

Ref. Kalogera & Baym, ApJ **470** (1996) L61.

Many-body perturbation calculations with chiral 2N, 3N, 4N interactions

Hierarchy of nuclear forces in chiral perturbation theory:

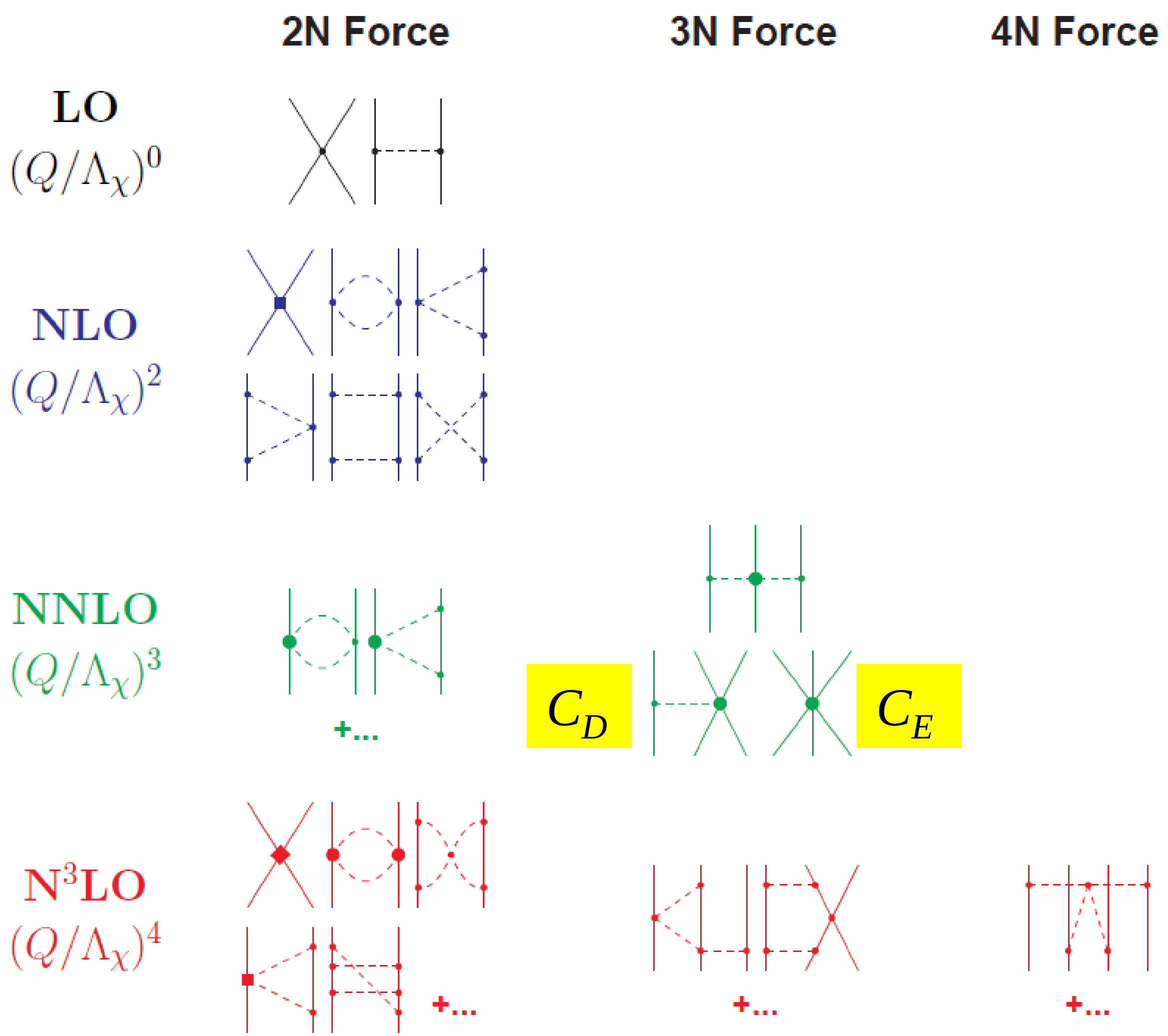

Figure 1: Hierarchy of nuclear forces in ChPT. Solid lines represent nucleons and dashed lines pions. Small dots, large solid dots, solid squares, and solid diamonds denote vertices of index $\Delta = 0, 1, 2,$ and 4, respectively. Further explanations are given in the text.

Ref. Machleidt & Entem, arXiv:1105.2919.

Many-body perturbation calculations with chiral 2N, 3N, 4N interactions

1st, 2nd, 3rd order pp and 3rd ph contributions due to 2N interactions:

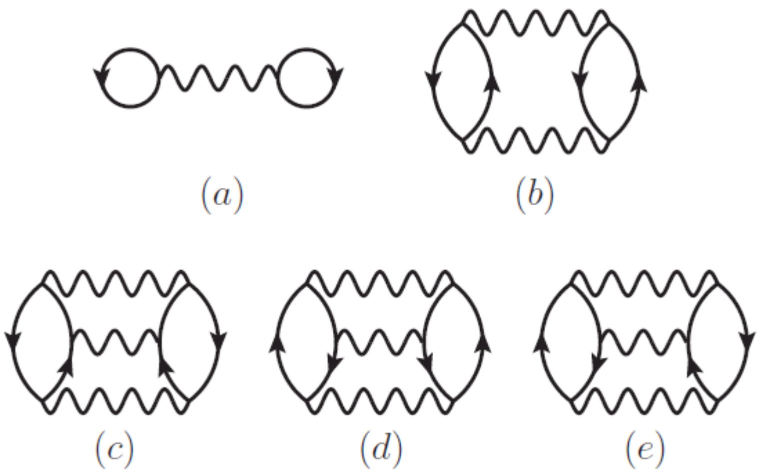

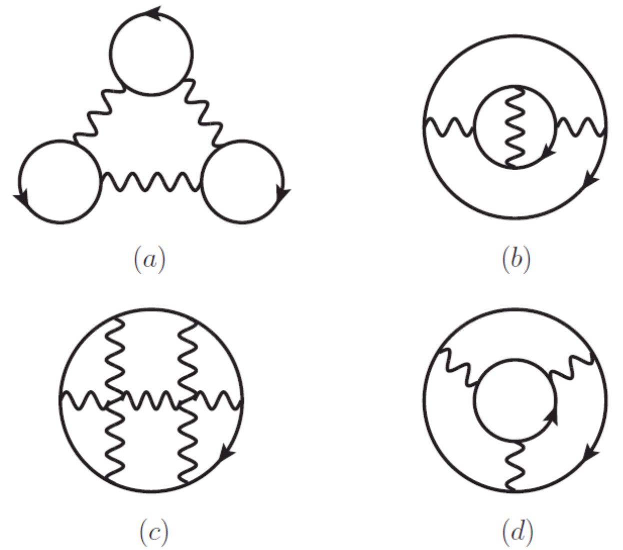

Ref. Holt & Kaiser, PRC **95** (2017) 034326.

1st, 2nd order pp contributions due to 3N and 4N interactions:

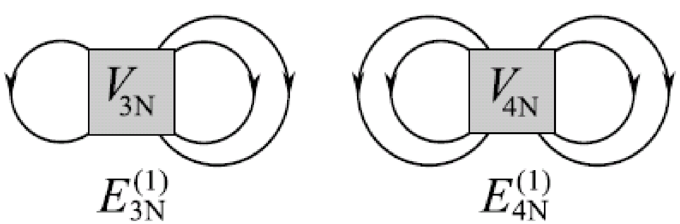

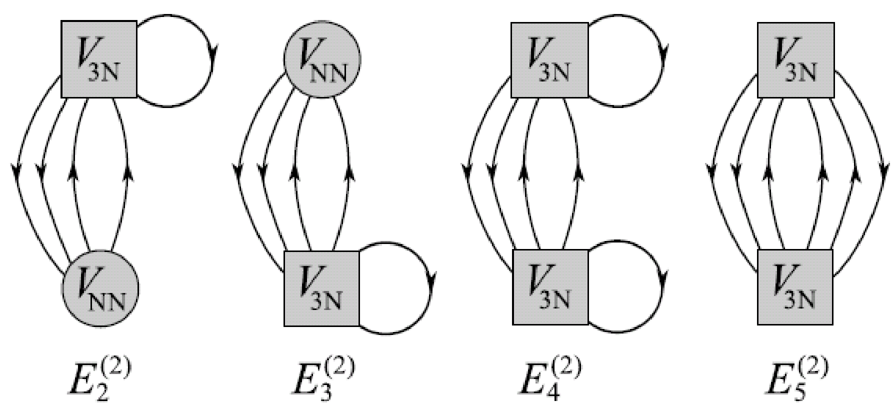

Ref. Krüger, Tews, Hebeler, & Schwenk, PRC **88** (2013) 025802.

Many-body perturbation calculations with chiral 2N, 3N, 4N interactions

Up to 4^{th} order:

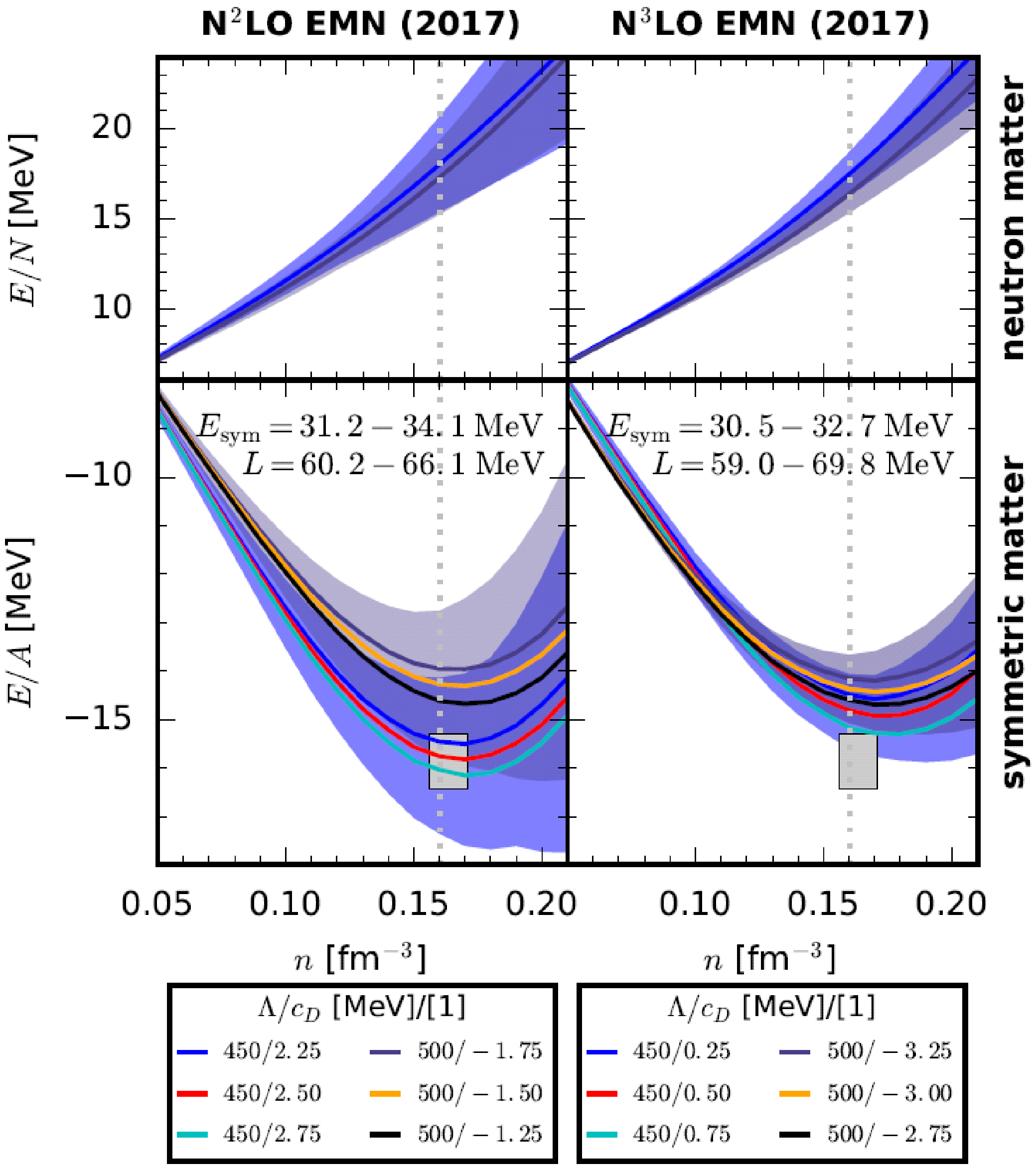

3N interaction parameters fitted to the empirical saturation region and triton binding energy

Ref. Drischler, Hebeler, & Schwenk, arXiv:1710.08220.

1.97Msun neutron star

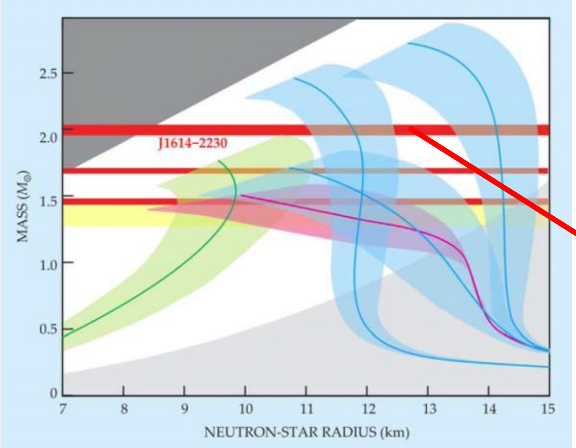

Demorest et al. (2010)

What is the real EOS of neutron star matter?

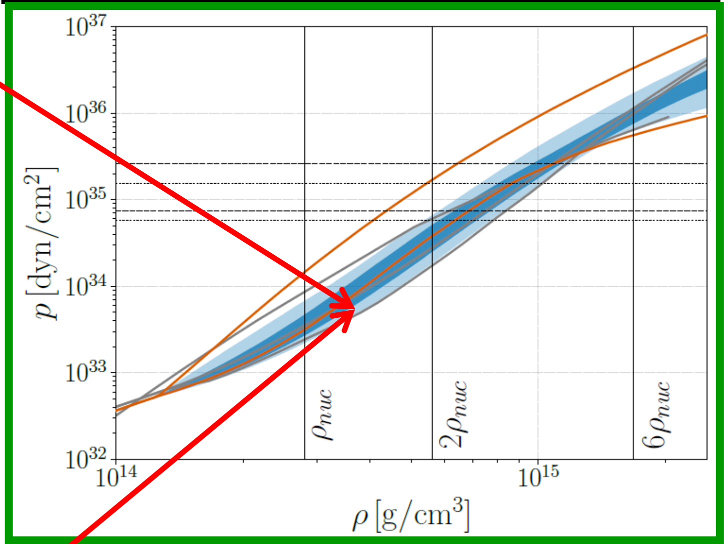

Lattice QCD calculations at finite density in principle could give the real EOS and phase diagram, but in practice are faced by the sign problem.

GW170817 (NS-NS merger)

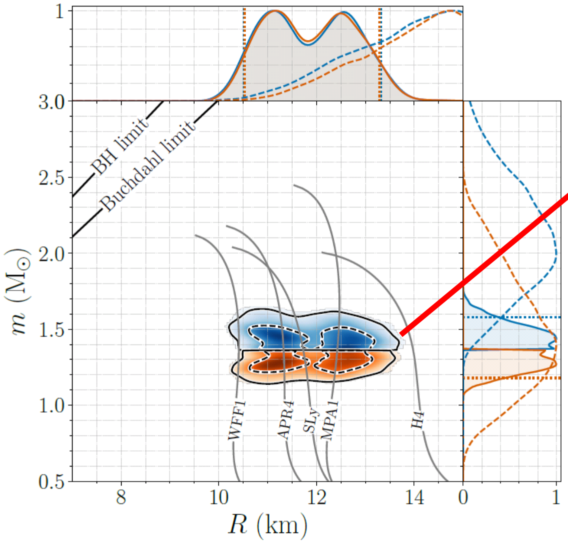

LIGO & Virgo, arXiv:1805.11581.

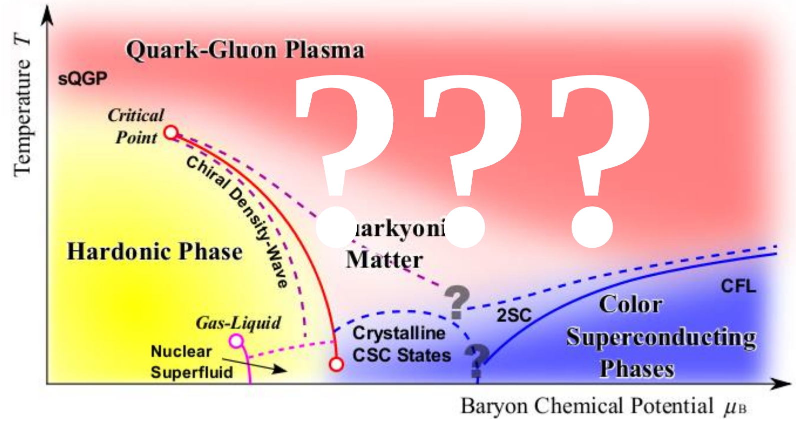

By Fukushima

Lucky stars

The neutron star created in a merger was traced as it lost its fast-spinning outer layers, spun as a rigid body, then collapsed into a black hole. That allowed researchers to infer the maximum mass of a stable neutron star.

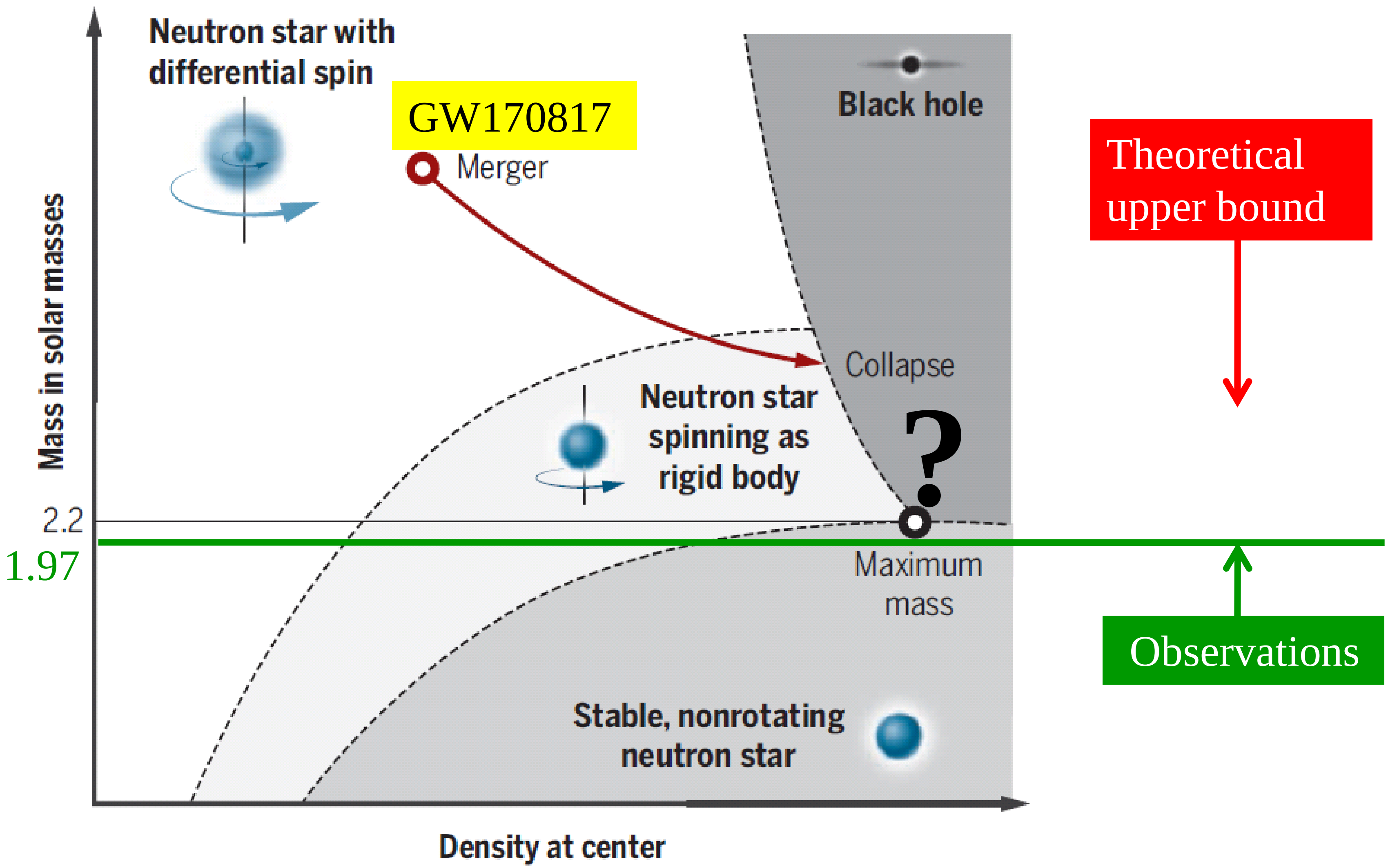

Ref. A. Cho, Sci. **359** (2018) 724.

Conclusion

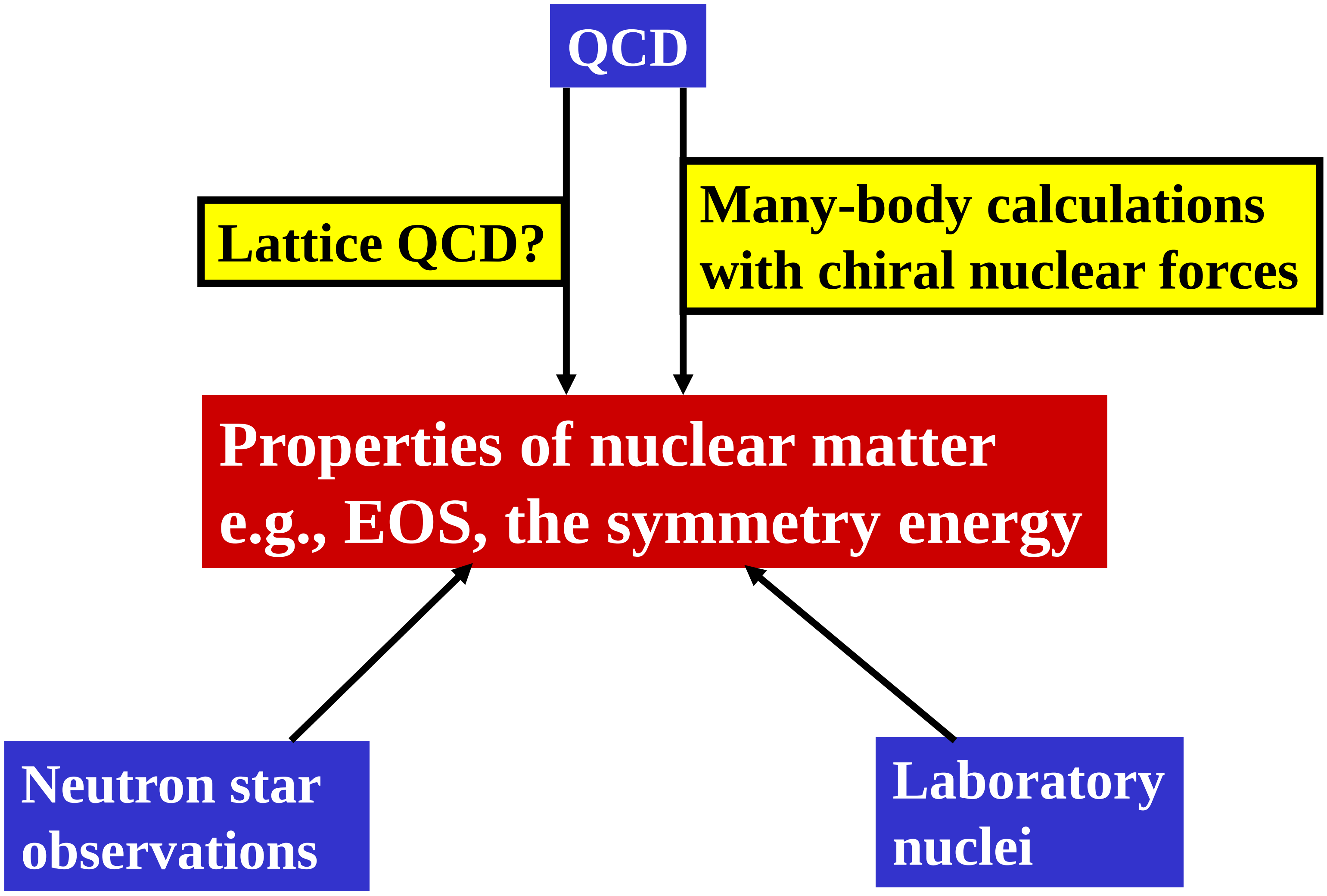
QCD
Lattice QCD?
Many-body calculations with chiral nuclear forces
Properties of nuclear matter e.g., EOS, the symmetry energy
Neutron star observations
Laboratory nuclei